April 25, 2016

# SUBJECTIVE AND OBJECTIVE QUALITY EVALUATION OF SYNTHETIC AND HIGH DYNAMIC RANGE IMAGES

Ms. Debarati Kundu

Ph.D. Defense

Prof. Alan C. Bovik
Prof. Brian L. Evans (Supervisor)
Prof. Donald S. Fussell
Prof. Wilson S. Geisler III
Prof. Joydeep Ghosh

The University of Texas at Austin
Electrical and Computer Engineering
Cockrell School of Engineering

Wireless Networking & Communications Group

Embedded Signal Processing Laboratory
ESPL
The University of Texas at Austin

# Outline

- Introduction
- Image Quality Evaluation of Synthetic Scenes
- Image Quality Evaluation of High Dynamic Range Scenes
- Conclusion

Synthetic Scene

High Dynamic Range Scene

# Motivation

- Natural images captured by optical cameras
  - 350M photos are uploaded to Facebook every day on average
- Computer graphics generated content
  - Massively multiplayer online gaming (23.4M subscribers worldwide)
  - Animated movies and synthetic still images
- High Dynamic Range Images
  - Capturing HDR images in recent cellphones (e.g. iPhones)
  - Displaying HDR videos for home (e.g. Samsung)
  - Streaming HDR content (e.g. Amazon Video, Netflix)
- **Image Quality Assessment very important**

Source: Statista.com

# Image Quality Assessment (IQA) Algorithms

Reference

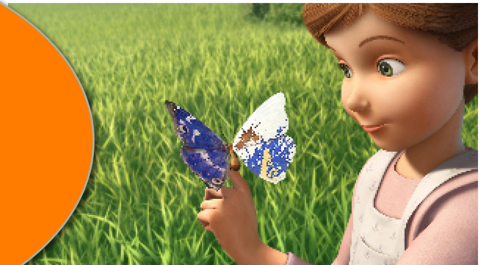

Test

**"Full-Reference" (FR) IQA** require an "original"high quality image for **comparison**.

**"No-Reference" (NR) IQA** assume that **no "original image"** is available for **comparison**.

**"Reduced-Reference" (RR) IQA** require supplementary information about the original image

Supplemental Information

Full Reference IQA

Reduced Reference IQA

No-Reference IQA

Subjective Opinion Scores

Correlation

Performance

[Dr. Alan C. Bovik, EE381V Digital Video, Spring 2015]

# Thesis Statement and Contributions

**Thesis Statement**

Using scene statistics yields automatic visual quality assessment algorithms for synthetic images and high dynamic range images that have high correlation with human visual quality evaluation.

- Image Quality Evaluation of Synthetic Scenes
  1. Subjective Experiment
  2. Objective Quality Evaluation
- Image Quality Evaluation of High Dynamic Range Scenes
  3. Evaluation of Full-Reference Measures
  4. Crowdsourced Subjective Study
  5. Proposed No-reference Quality Measures

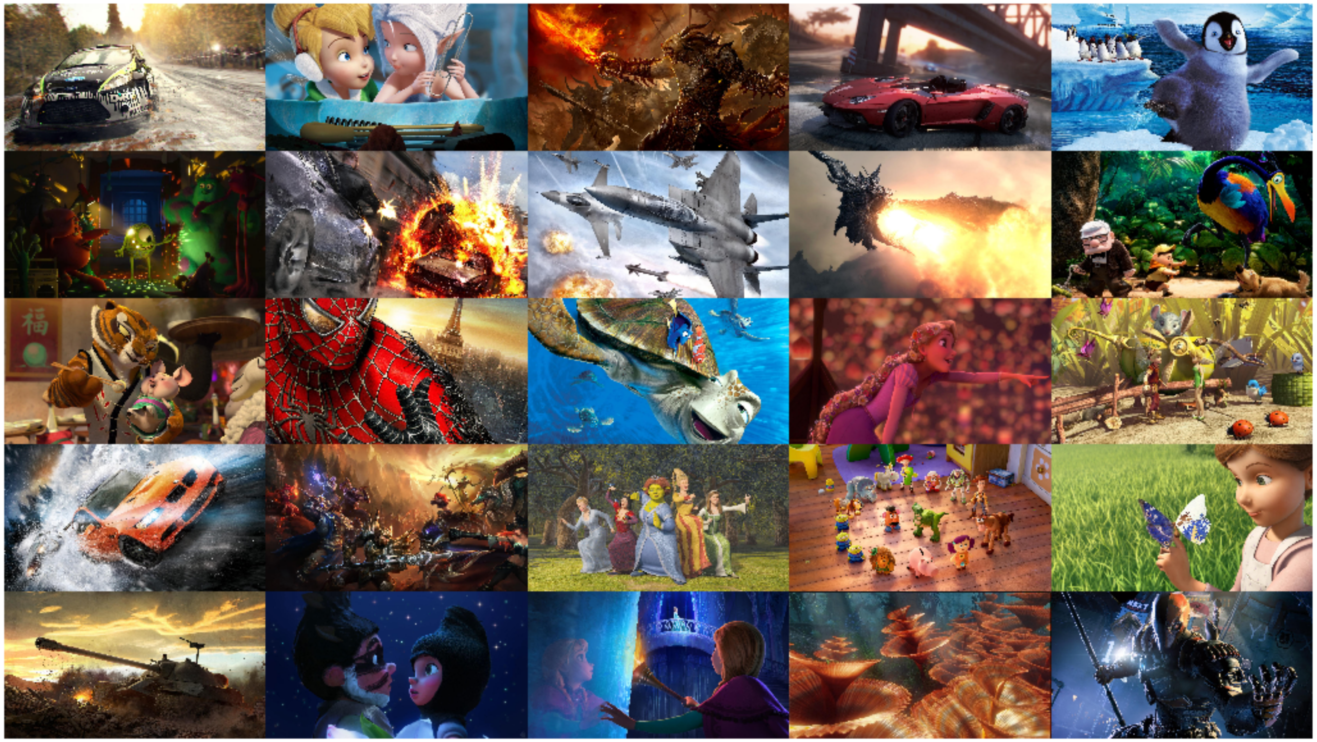

# Image Quality Evaluation of Synthetic Scenes

*"I learned that realism can come in all shapes and sizes. The world is big enough for different values to coexist."*
*— Haruki Murakami, The Folklore of Our Times*

# ESPL Synthetic Image Database[Kundu2015]

- 25 reference images + 500 distorted images
- 5 distortion categories, 4 levels of each distortion
- Single Stimulus Continuous Quality Scale (0-100) with hidden reference
- 52 observers: 12 among 64 subjects removed as outliers
- Annotated images with differential mean opinion scores (DMOS)
- Website: http://signal.ece.utexas.edu/~bevans/synthetic/

Reference (DMOS = 0)

Distorted (DMOS = 74.68)

# ESPL Database: Distortions

Interpolation
(DMOS = 63.23)

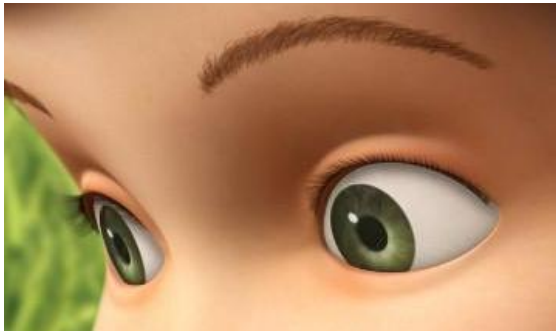

**Original**
**(DMOS = 0)**

JPEG Compression
(DMOS = 74.68)

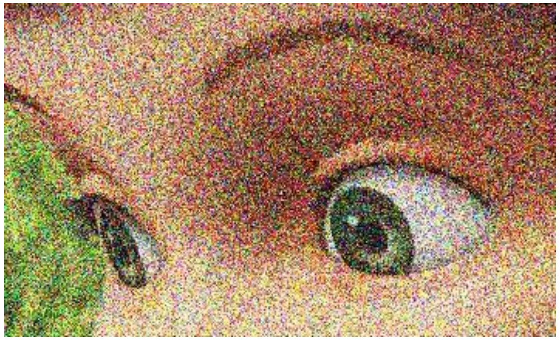

Additive Noise
(DMOS = 60.33)

Blur
(DMOS = 50.89)

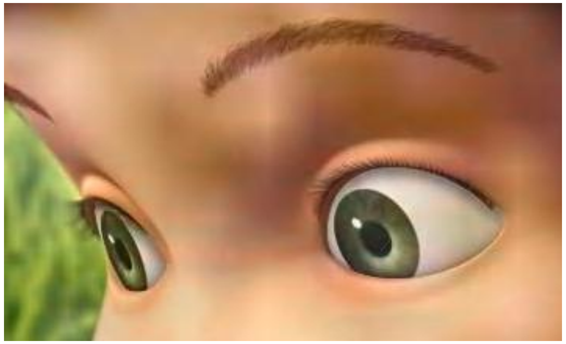

Fast Fading
(DMOS = 60.26)

Considered less severe distortions compared to what appears in natural images

# ESPL Objective IQA: Correlation between DMOS and IQA scores

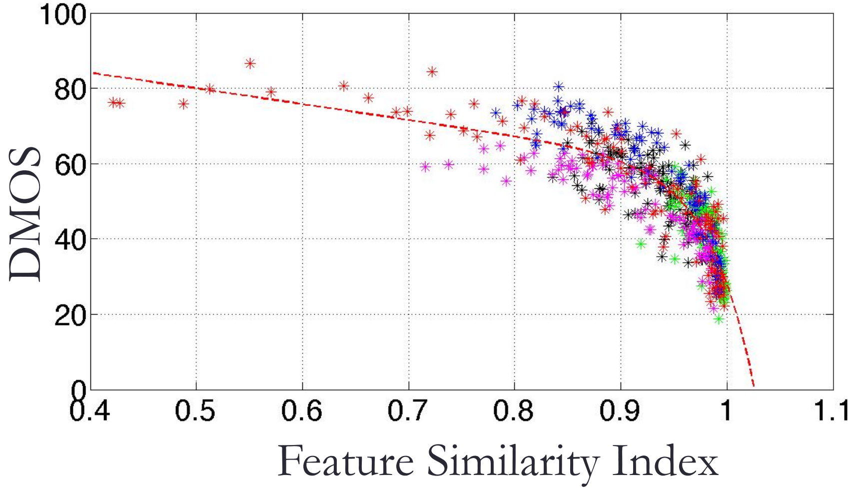


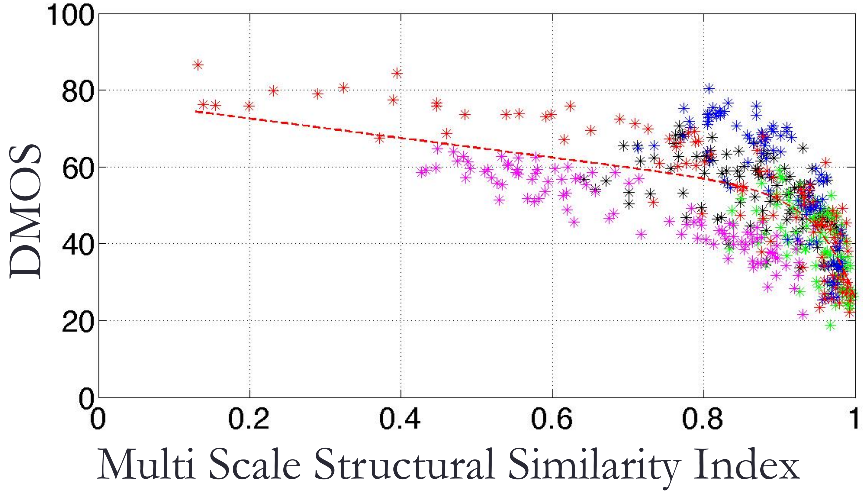


Scatter plot of two IQA algorithms vs. DMOS scores


- IQA algorithms evaluated for correlation with human scores
- Different correlation measures:
  - Spearman Rank Order Correlation Coefficient (SROCC)
  - Pearson Linear Correlation Coefficient (PLCC)
- Non-linear regression on objective IQA scores with logistic function

# ESPL Objective IQA: SROCC for Full-Reference IQAs

| Algorithms | Inter-polation | Blur | Additive Noise | JPEG Blocking | Fast Fading | Overall |
|---|---|---|---|---|---|---|
| GMSD | 0.727 | **0.827** | **0.923** | 0.918 | 0.922 | **0.892** |
| SR-SIM | 0.752 | **0.823** | **0.916** | 0.925 | 0.920 | **0.880** |
| FSIM | 0.692 | 0.801 | 0.902 | **0.940** | 0.907 | 0.876 |
| MAD | **0.788** | 0.813 | 0.909 | 0.933 | **0.927** | 0.863 |
| SSIM-D | 0.688 | 0.772 | 0.915 | 0.914 | 0.904 | 0.796 |
| MS-SSIM | 0.623 | 0.646 | 0.908 | 0.871 | 0.903 | 0.699 |
| PSNR | 0.565 | 0.481 | 0.864 | 0.695 | 0.846 | 0.590 |
| SSIM | 0.463 | 0.440 | 0.909 | 0.633 | 0.797 | 0.542 |

- GMSD: Gradient Magnitude Similarity Deviation [Xue2014]
- SR-SIM: Spectral Residual based Similarity Index [Zhang2012]
- FSIM: Feature Similarity Index [Zhang2011]
- MAD: Most Apparent Distortion Index [Larson2010]
- MS-SSIM: Multiscale-Structural Similarity Index [Wang2003]
- PSNR: Peak Signal-to-Noise Ratio [Wang2003]
- SSIM: Structural Similarity Index Metric [Wang2003]

No-reference

# ESPL Objective IQA: Some insights

- PSNR outperforms SSIM for all distortio
  - Need to choose appropriate scale for SSIM
  - Some users rated distorted image higher than reference

max(1,round(N/256))
N = Minimum image dimension

- Challenging distortions
  - Presence of blur may not always correspond to a lower subjective score
  - Interpolation caused near-threshold artifacts for low upsampling factors
- Efficient pooling strategies across image subblocks play important role

22 among 52 subjects rated the blurred version higher than the original one

Reference (DMOS = 0)

Blurred (5x5 Gaussian kernel. σ = 1.25 pixels) (DMOS = 18.86)

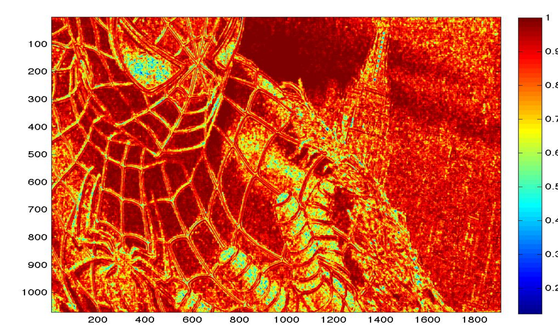


SSIM map

# ESPL Objective IQA: Synthetic Scene Statistics

- Natural Scene statistics
  - Natural pristine images have statistics that occur irrespective of content
  - Statistics of images with distortions deviate from NSS
- Mean Subtracted Contrast Normalized (MSCN) pixels [Ruderman1993]
  - Models divisive normalization in human visual systems
  - Let $I(i,j)$ be the pixel located at $(i,j)$th spatial location
  - MSCN, $\hat{I}(i,j) = \dfrac{I(i,j) - \mu(i,j)}{\sigma(i,j) + 1}$
  - Mean $\mu(i,j) = \sum_{k=-K}^{K} \sum_{l=-L}^{L} w_{k.l} I(i+k, j+l)$
  - Standard deviation $\sigma(i,j) = \sqrt{\sum_{k=-K}^{K} \sum_{l=-L}^{L} w_{k.l} [I(i+k, j+l) - \mu(i,j)]^2}$

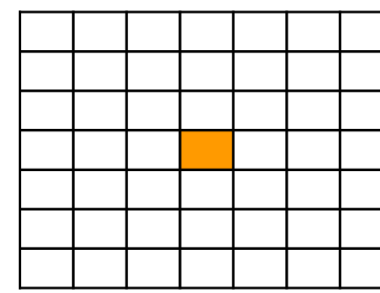

7x7 window size for local statistics

$W_{k,l}$: Gaussian Weighting Factor

# ESPL Objective IQA: SROCC for No-reference IQAs

| Algorithms | Interpolation | Blur | Additive Noise | JPEG Blocking | Fast Fading | Correlation |
|---|---|---|---|---|---|---|
| G-IQA-1(L) | 0.605 | 0.612 | 0.858 | 0.908 | **0.774** | **0.813** |
| CORNIA | **0.808** | **0.775** | 0.793 | 0.898 | 0.706 | 0.810 |
| C-DIIVINE | 0.702 | 0.730 | 0.847 | 0.841 | 0.738 | 0.798 |
| BRISQUE | 0.631 | 0.720 | 0.840 | 0.898 | 0.717 | 0.789 |
| DESIQUE | 0.595 | 0.590 | **0.886** | **0.934** | 0.714 | 0.773 |

- G-IQA-1(L): Gradient Image Quality Assessment-1 (Luminance) [Kundu2016]
- CORNIA: Codebook Rep for No-Ref Image Assessment (CORNIA) [Ye2012]
- C-DIIVINE: Complex Distortion Identification-based Image Verity and INtegrity Evaluation [Zhang2014]
- BRISQUE: Blind/Referenceless Image Spatial Quality Evaluator [Mittal2012]
- DESIQUE: DErivative Statistics-based Quality Evalulator [Zhang2013]

Full-reference

# Full-reference Image Quality Evaluation of HDR Images

*"It is a part of probability that many improbabilities will happen."*
*— Aristotle*

# HDR creation pipeline

Tonemapping

Estimate radiance map by merging pixels from different exposures

Tonemap floating point irradiance map to SDR

Post-processing

Merge SDR exposure stack directly to get fused image

Post-processing

Registered exposure stack

Multi-Exposure Fusion

# HDR Tone-mapping operators [Larson, 1997]

Uniformly spaced quantization of luminances overexposes the view through the window

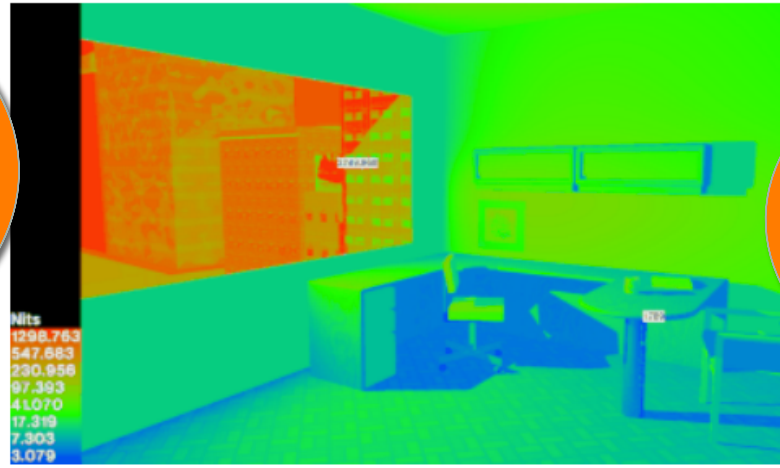


Luminances mapped to preserve visibility of both indoor & outdoor features using non-linear tone mapping

World luminance values for a window office in candelas per meter squared

# HDR IQA: Applications

Image quality assessment for HDR scenes for designing better

- Tone-mapping operators for standard dynamic range (SDR) displays
- Multi-exposure fusion algorithms
- Compression for HDR images (e.g., JPEG-XR)
- HDR rendering for computer graphics

Multi-exposure fusion

HDR rendering

# Full-Reference IQA for Tonemapping

- Previous FR-IQA algorithms for tone mapping distortions
  - Tone Mapped Quality Index (TMQI): inspired by SSIM [Yeganeh2013]
  - Feature Similarity Index for Tone Mapped Images (FSITM): based on phase congruency [Nafchi2014]
- Image saliency by pooling IQA scores in each subblock
  - Attention based on Information Maximization based TMQI[Nasrinpour2015]
  - Itti and Koch's method generalized for HDR applications [Petit2010]
  - Simpler weighting measures needed for faster execution speed
- Finding better Natural Scene Statistics models to quantify "naturalness"
- Designing algorithms for other types of HDR distortions
  - Compression of HDR images

# Spatial domain statistics for tonemapping

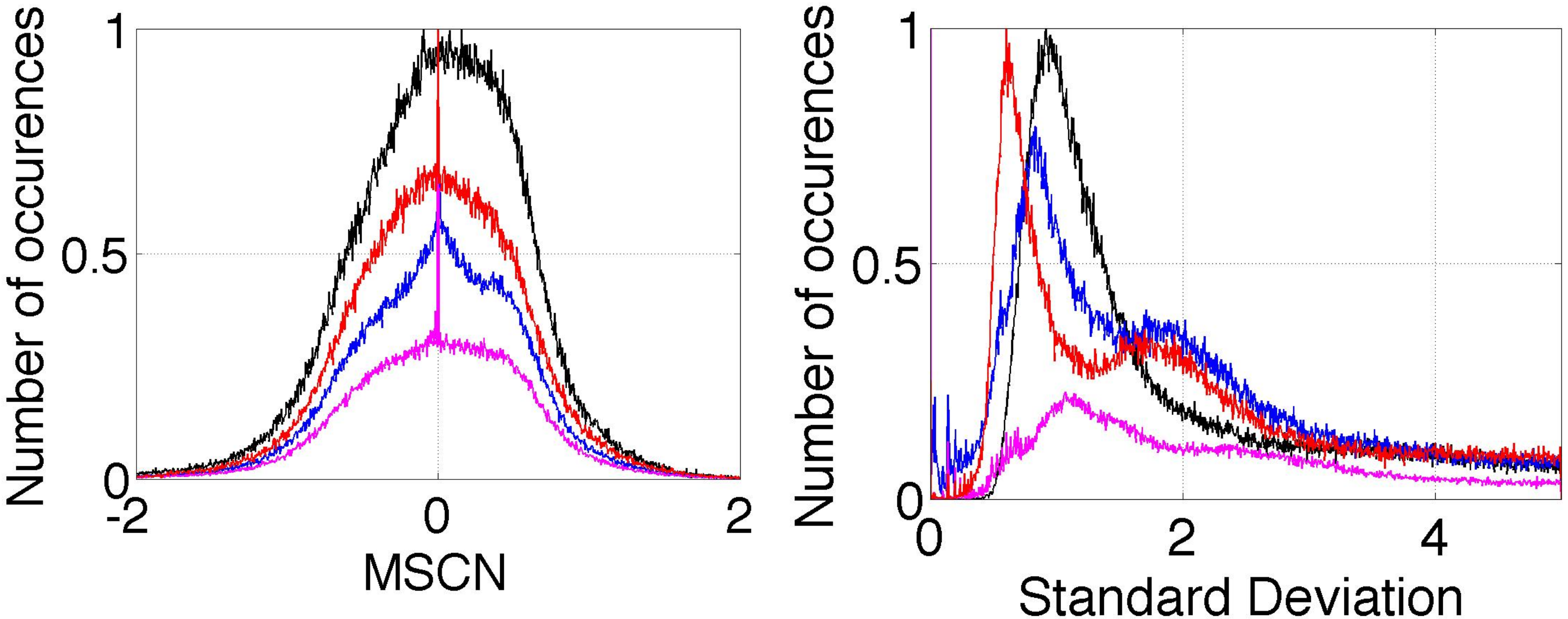


MSCN coefficient distribution and σ-field distribution for different tone-mapping operators

# HDR IQA: MSCN based Scene Statistics

- Multiscale TMQI yield structural fidelity score (S)
- Proposed combination of structural fidelity and naturalness scores:

$$Q = aS^{\gamma} + \frac{1}{2}(1-a)\beta^{\delta_1} + \frac{1}{2}(1-a)\phi^{\delta_2}$$

- β: Scale parameter of GGD fit of MSCN coefficients
- ϕ: Standard deviation of the σ-field
- $\gamma, \delta_1, \delta_2$ are the sensitivity parameters
- $a$ indicates relative weighting of the terms

# HDR IQA: Local pooling techniques

- Average pooling gives same importance to every pixel.
- Two non-uniform pooling strategies:
  - σ-map
  - Local entropy
- σ-map gives measure of edge magnitude and high contrast regions
- Local entropy indicates local randomness

Tone mapped image

Structural fidelity map

Structural fidelity with pooling

# HDR IQA: TMQI Database Results [Yeganeh2013]

- 15 source HDR images
- Each HDR image mapped to SDR using 8 tone-mapping operators.
- Subjects ranked these 8 SDR images for every source image

| FR-IQA Algorithms | SROCC | PLCC | Time(s) |
| --- | --- | --- | --- |
| TMQI-NSS-Sigma (Proposed) | **0.8810** | **0.9439** | 0.3212 |
| TMQI-NSS-Entropy (Proposed) | **0.8810** | 0.9438 | 1.2759 |
| TMQI-Itti (Proposed) | **0.8810** | 0.9346 | 0.8010 |
| FSITM-TMQI[Nafchi2014] | 0.8571 | 0.9230 | 0.9428 |
| STMQI[Nasrinpour2015] | 0.8503 | 0.9382 | 1.538 |
| TMQI-II[Ma2015] | 0.8333 | 0.8790 | **0.2002** |
| Feature Similarity Index for Tone-Mapped Images(FSITM) [Nafchi2014] | 0.8333 | 0.8948 | 0.4741 |
| Tone Mapped Image Quality Index (TMQI)[Yeganeh2013] | 0.8095 | 0.9082 | 0.5206 |

Correlation measures are computed between predicted ranks of tone-mapped images and ground-truth rankings for each source image. Result shows median of correlations computed.

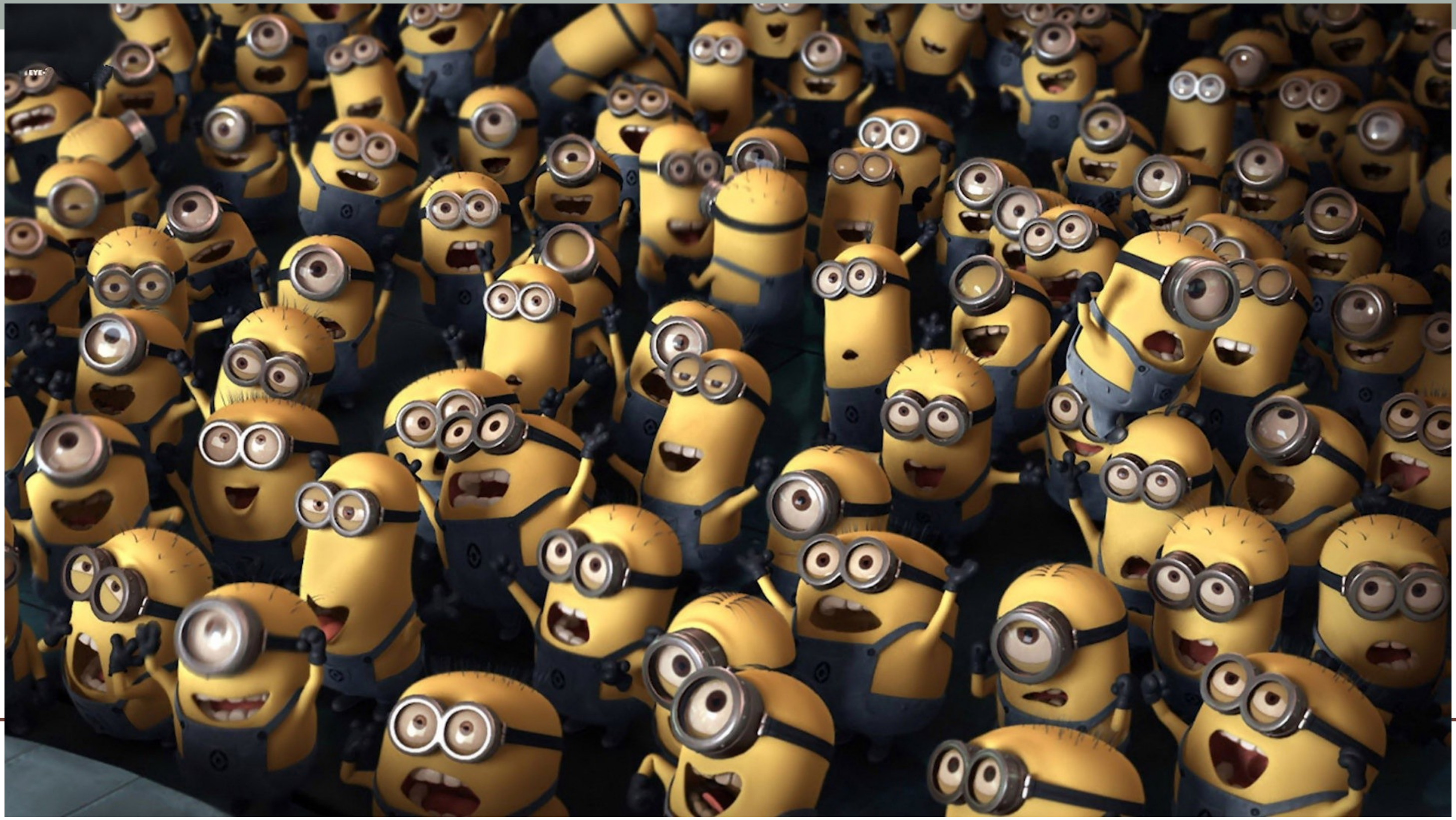

# Crowdsourced Study of High Dynamic Range Images

*"The desert has its holiness of silence, the crowd its holiness of conversation."*
*— Walter Elliot*

# HDR-IQA: ESPL-LIVE Image Database

- 1,811 HDR images obtained from 605 source scenes
- Size: 960x540 for landscape and 540x304 for portrait orientation
- Single Stimulus Continuous Quality Scale (0-100)
- 327,720 raw quality scores from 5,462 subjects
- Images annotated with mean opinion scores (MOS)

Sample images

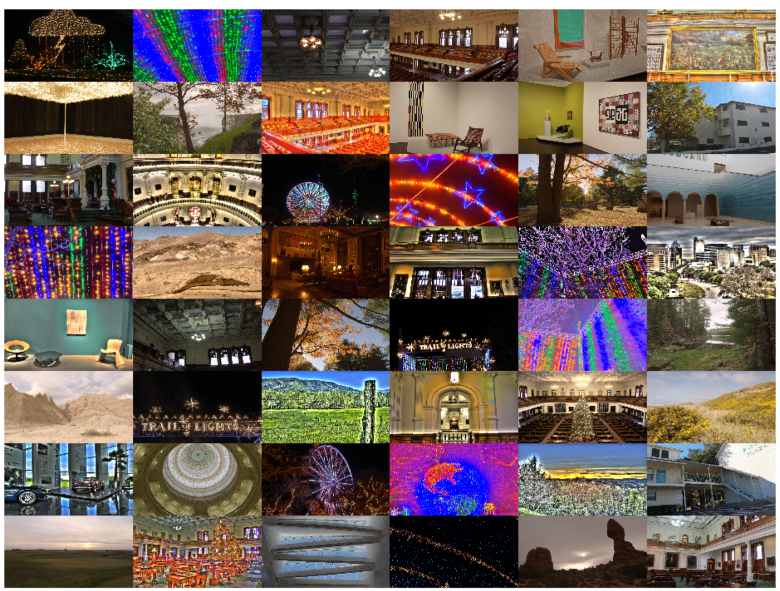

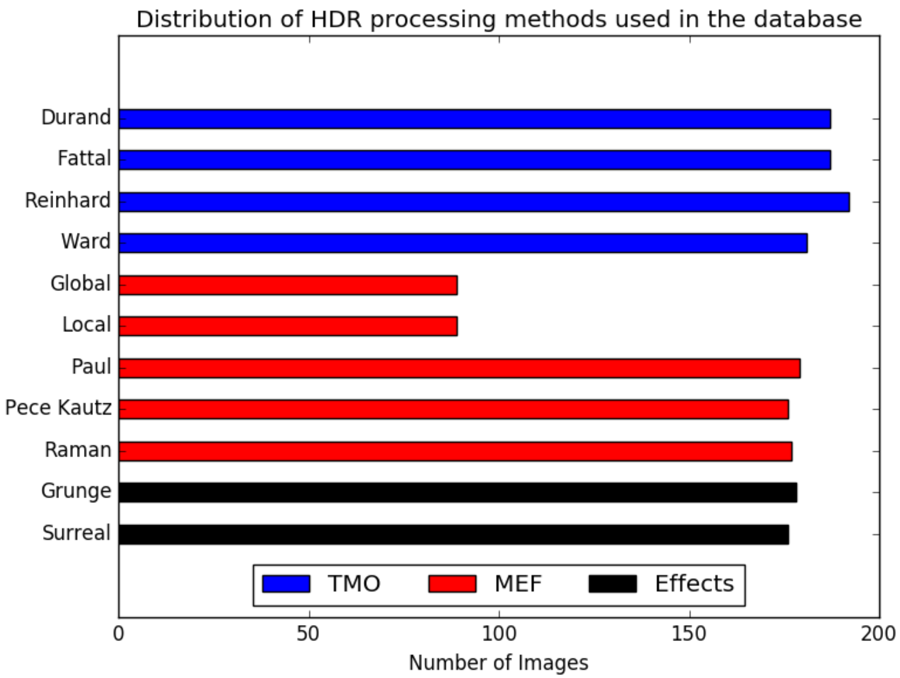

# HDR-IQA: Subjective Testing Methodology

- 12 subjects evaluated 27 images in laboratory setting
  - 5 'Gold Standard' images
- Amazon Mechanical Turk used for crowdsourcing
  - Training images: 11
  - Test images: 49
  - 'Gold Standard' images: 5 (Viewed by every subject)
  - Randomly repeated images : 5
- At the end subjects answered questions on demographics, display parameters, and familiarity with HDR imaging


Source: Amazon.com

# HDR-IQA: Processing of the raw scores

- Subject rejection strategies:
  - Only subjects with AMT confidence values greater than 0.75 participated
  - If scores assigned to multiple copies of the same image differed by more than 25.5 for three images, scores from that user was rejected
  - 388 subjects among 5,462 removed as outliers
- Processing of remaining scores:
  - On an average, every image evaluated by 110 subjects
  - Mean Opinion Scores: Mean of Z-score for every image
  - Spans 16.941 - 68.502.
  - Raw MOS scores span 5.623 – 84.661
- Consistency with laboratory setting:
  - Median PLCC between individual scores and MOS values for 'Gold Standard' images in laboratory setting was **0.9466**

Details

# No-reference Image Quality Assessment Algorithm for High Dynamic Range images

*"An algorithm must be seen to be believed."*
*— Donald Knuth*

# HDR IQA: MSCN and local $\sigma$ -map distributions

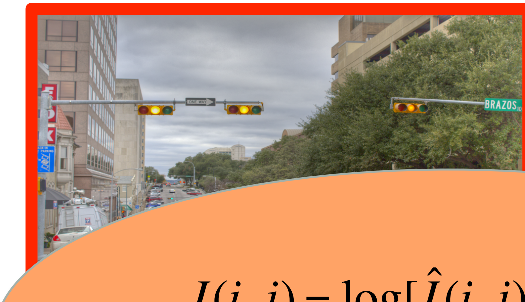

(a) MOS = 40.47

52.80

$$J(i,j) = \log[\hat{I}(i,j) + K]$$

$$\nabla_x J(i,j) = J(i,j+1) - J(i,j)$$

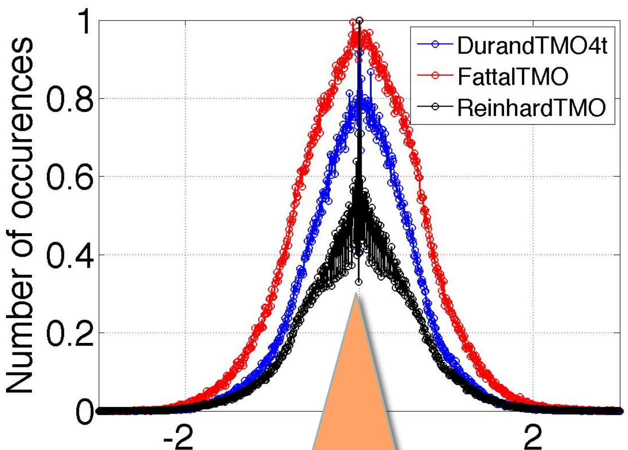


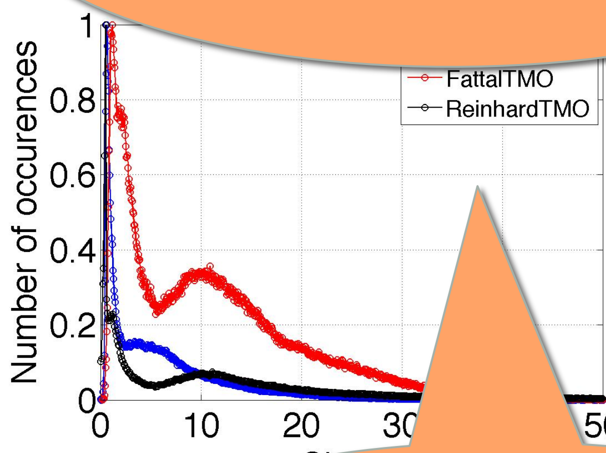


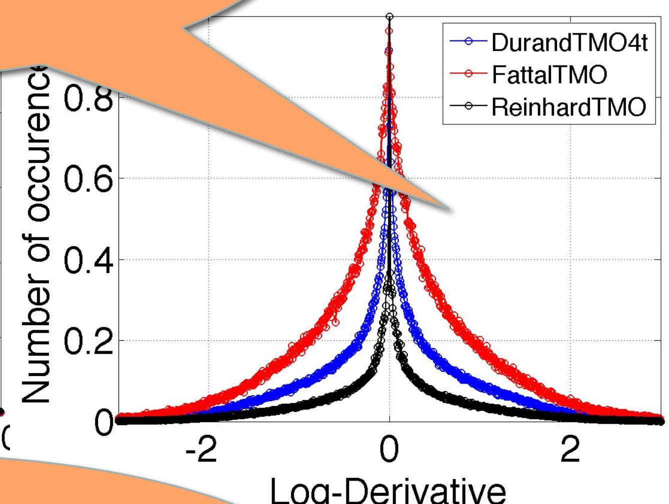


$$\hat{I}(i,j) = \frac{I(i,j) - \mu(i,j)}{\sigma(i,j) + 1}$$

$$\sigma(i,j) = \sqrt{\sum_{k=-K}^{K} \sum_{l=-L}^{L} w_{k.l} \left[ I(i+k, j+l) - \mu(i,j) \right]^2}$$

# HDR IQA: Distribution of gradient domain features



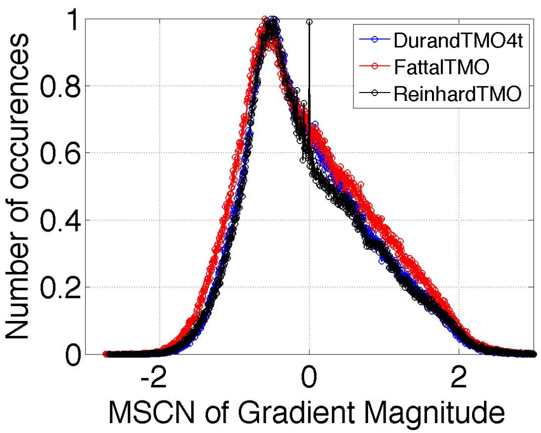


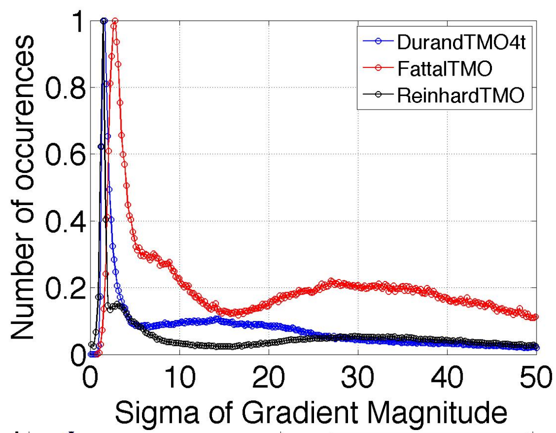


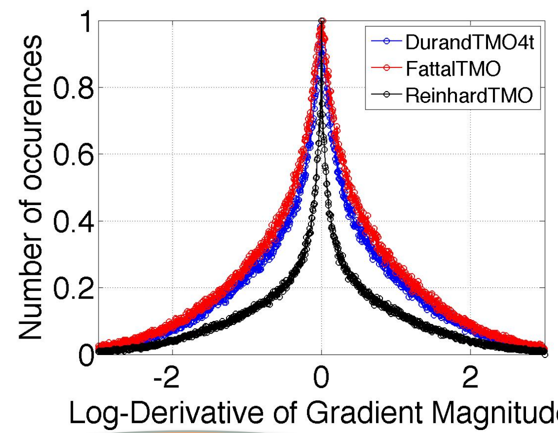


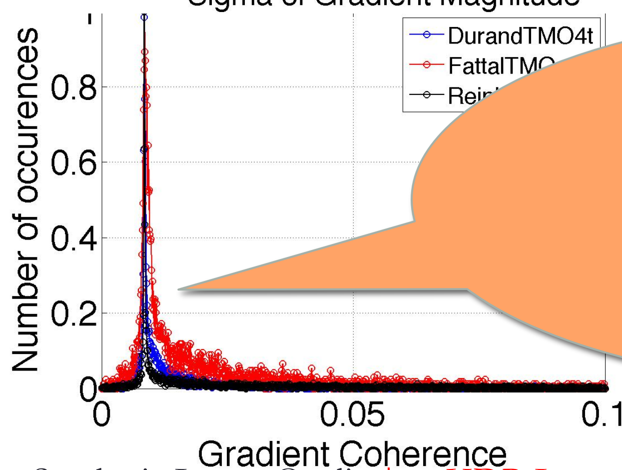


$$J = \begin{bmatrix} f(G_x) & f(G_xG_y) \\ f(G_xG_y) & f(G_y) \end{bmatrix}$$

$$C = \left(\frac{\lambda_1 - \lambda_2}{\lambda_1 + \lambda_2}\right)^2$$

# HDR IQA: SROCC between each feature and MOS

| Domain | Feature Description | SROCC |
|---|---|---|
| Spatial [f1 – f2] | Shape and Scale parameters of AGGD fitted to MSCN coefficients | 0.238 |
| Spatial [f3 – f16] | Shape and Scale parameters of AGGD fitted to log-derivative of the seven types of neighbors | **0.439** |
| Spatial [f17 – f18] | Mean and standard deviation based features extracted from the $\sigma$ -field | 0.369 |
| Gradient [f19 – f20] | Shape and Scale parameters of the AGGD fitted to the MSCN coefficients of gradient magnitude field | 0.250 |
| Gradient [f21 – f34] | Shape and Scale parameters of AGGD fitted to log-derivative of seven types of neighbors of gradient magnitude field | 0.386 |
| Gradient [f35 – f36] | Mean and standard deviation based features extracted from the $\sigma$ -field of gradient magnitude field | 0.388 |
| Gradient [f37 – f40] | Mean, standard deviation, skewness, and kurtosis of gradient structure tensor coherence | 0.420 |

G-IQA-1: [f1 – f36]

G-IQA-2: [f1 – f18, f37 f40]

Features computed across 2 levels and in LAB color space

# ESPL-LIVE HDR objective IQA: No-reference SROCC

- Computed on ratings obtained from 4,715 subjects
- 80% training, 20% testing, 100 random train-test splits
- No content overlap to prevent artificial inflation of correlations

More

| Algorithms | Tone Mapping | Multi Exposure Fusion | Post Processed | Overall |
|---|---|---|---|---|
| G-IQA-1 | 0.692 | 0.691 | **0.582** | **0.716** |
| G-IQA-2 | **0.720** | **0.698** | 0.484 | 0.709 |
| G-IQA-1 (L) | 0.651 | 0.623 | 0.489 | 0.662 |
| G-IQA-2 (L) | 0.661 | 0.631 | 0.419 | 0.656 |
| DESIQUE | 0.503 | 0.550 | 0.476 | 0.565 |
| GM-LOG | 0.521 | 0.521 | 0.527 | 0.562 |
| CurveletIQA | 0.542 | 0.512 | 0.435 | 0.546 |
| DIIVINE | 0.485 | 0.456 | 0.335 | 0.480 |
| BLIINDS-II | 0.385 | 0.421 | 0.435 | 0.448 |
| BRISQUE | 0.267 | 0.431 | 0.431 | 0.402 |

# Conclusion

**Thesis Statement**

Using scene statistics yields automatic visual quality assessment algorithms for synthetic images and high dynamic range images that have high correlation with human visual quality evaluation.

- Image Quality Evaluation of Synthetic Scenes
  1. Designed ESPL Synthetic Image Database
  2. Compared performance of state-of-the-art IQA algorithms for synthetic images
- Image Quality Evaluation of High Dynamic Range Scenes
  3. Used scene statistics and visual saliency measures for full-reference evaluation of HDR scenes
  4. Conducted a large scale subjective study for HDR images
  5. Proposed scene-statistics based NR-IQA algorithms for HDR images

# Relevant Publications

- D. Kundu and B. L. Evans, "Spatial Domain Synthetic Scene Statistics", *Proc. Asilomar Conf. on Signals, Systems, and Computers*, Nov. 2-5, 2014, Pacific Grove, CA USA.
- D. Kundu and B. L. Evans, "Full-reference visual quality assessment for synthetic images: A subjective study", in *Proc. IEEE Int. Conf. on Image Processing*, September 2015. **Won Top 10% Paper Award.**
- D. Kundu and B. L. Evans, "No-reference synthetic image quality assessment using scene statistics," in *Proc. Asilomar Conf. Signals, Systems and Computers.*, November 2015.
- D. Kundu, L. K. Choi, A. C. Bovik and B. L. Evans, ``Subjective and Objective Quality Evaluation of Lightly Distorted Synthetic Images", *IEEE Transactions on Image Processing*, to be submitted.
- D. Kundu and B. L. Evans, "Visual Attention Guided Quality Assessment of Tone-Mapped Images using Scene Statistics", submitted to *IEEE Int. Conf. on Image Processing*, September 2016.

# Questions?


THANK
YOU
GRACIAS
ARIGATO
SHUKURIA
DANKSCHEEN
BIYAN
SHUKRIA
TINGKI
YAQHANYELAY
TASHAKKUR ATU
SUKSAMA
EKHMET
MEHRBANI
GRAZIE
MAAKE
KOMAPSUMNIDA
GOZAIMASHITA
EFCHARISTO
JUSPAXAR
PALDIES
BOLZÏN
MERCI

# References


- [Bremond2010] J. Petit, R. Bremond, and J.-P. Tarel, "Saliency maps of high dynamic range images," in Proceedings of the 6th Symposium on Applied Perception in Graphics and Visualization , ser. APGV '09. New York, NY, USA: ACM, 2009.
- [Ferwerda2007] G. Ramanarayanan, J. Ferwerda, B. Walter, and K. Bala, "Visual equivalence: Towards a new standard for image fidelity," in SIGGRAPH ACM, 2007
- [Ghadiyaram2016] D. Ghadiyaram and A. C. Bovik, "Massive Online Crowdsourced Study of Subjective and Objective Picture Quality," IEEE Trans. Img. Proc. vol. 25, no. 1, Jan. 2016
- [Kundu 2014] D. Kundu and B. L. Evans, ``Spatial Domain Synthetic Scene Statistics", Pro c. Asilomar Conf. on Signals, Systems, and Computers, Nov. 2-5, 2014, Pacific Grove, CA USA.
- [Kundu2015] D. Kundu and B. L. Evans, ``Full-Reference Visual Quality Assessment for Syn thetic Images: A Subjective Study", Proc. IEEE Int. Conf. on Image Processi ng, Sep. 27-30, 2015, Quebec City, Canada. [Larson1997] G. W. Larson, H. Rushmeier, and C. Piatko. 1997. A Visibility Matching Tone Reproduction Operator for High Dynamic Range Scenes. IEEE Transactions on Visualization and Computer Graphics 3, 4 (October 1997), 291-306.
- [Larson2010] E. C. Larson and D. M. Chandler, "Most apparent distortion: fullreference image quality assessment and the role of strategy," J Electronic Imaging, vol. 1 9, no. 1, p. 011006, 2010.
- [Ma2015] Kede Ma; Yeganeh, H.; Kai Zeng; Zhou Wang, "High Dynamic Range Image Compression by Optimizing Tone Mapped Image Quality Index," in Image Processing, IEEE Transactions on , vol.24, no. 10, pp.3086-3097, Oct. 2015
- [McGuire2012] M. McGuire, P. Hennessy, M. Bukowski, and B. Osman. 2012. A reconstruction filter for plausible motion blur. In Proceedings of the ACM SIGGRAPH Symposium on Interactive 3D Graphics and Games (I3D '12), ACM, New York, NY, USA, 135-142.

# References (cont'd)


- [Moorthy2011] A. K. Moorthy and A. C. Bovik, "Blind image quality assessment: From natural scene statistics to perceptual quality," IEEE Transactions on Image Processing, vol. 20, no. 12, pp. 3350– 3364, Dec 2011.
- [Nafchi2014] H. Ziaei Nafchi, A. Shahkolaei, R. Farrahi Moghaddam, and M. Cheriet, "Fsitm: A feature similarity index for tone-mapped images," Signal Processing Letters, IEEE , vol. 22, no. 8, pp. 1026-1029, Aug2015.
- [Narwaria2013] M. Narwaria, M. Perreira Da Silva, P. Le Callet, and R. Ppion, "Tone mapping-based high-dynamic-range image compression: study of optimization criterion and perceptual quality," Optical Engineering , vol. 52, no. 10, pp. pp. 102 008-1 102 008-15, Oct 2013.
- {Nasrinpour2015] 1 H. R. Nasrinpour and N. D. Bruce, "Saliency weighted quality assessment of tone-mapped images," in Proc. IEEE Int. Conf. on Image Process., Sept 2015, pp. 4947–4951.
- [Ruderman1993] D. L. Ruderman and W. Bialek, "Statistics of natural images: Scaling in the woods," in Neural Information Processing Systems Conference and Workshops, 1 993, pp. 551–558.
- [Saad2012] M. A. Saad, A. C. Bovik, and C. Charrier, "Blind image quality assessment: A natural scene statistics approach in the DCT domain." IEEE Transactions on Image Processing, vol. 21, no. 8, pp. 3339–3352, 2012
- [Wang2003] Z.Wang, E. P. Simoncelli, and A. C. Bovik, "Multiscale structural similarity for image quality assessment," in Proc. Asilomar Conference on Signals, Systems and Computers, vol. 2, Nov 2003, pp. 1398–1402 Vol.2.
- [Winkler2012] Winkler, S., "Analysis of Public Image and Video Databases for Quality Asses sment," in Selected Topics in Signal Processing, IEEE Journal of , vol.6, no .6, pp.616-625, Oct. 2012

# References (cont'd)

- [Xue2014] W. Xue, L. Zhang, X. Mou, and A. C. Bovik, \Gradient magnitude similarity deviation: A highly ecient perceptual image quality index," IEEE Trans. Image Process., vol. 23, no. 2, pp. 684-695, Feb 2014.
- [Xue2014] W. Xue, X. Mou, L. Zhang, A. C. Bovik, and X. Feng, "Blind image quality assessment using joint statistics of gradient magnitude and laplacian features," IEEE Transactions on Image Processing, vol. 23, no. 11, pp. 4850–4862, Nov 2014
- [Ye2012] Peng Ye, Jayant Kumar, Le Kang, and David Doermann, "Unsupervised Feature Learning Framework for No-reference Image Quality Assessment," in Proc. Intl. Conf. on Computer Vision and Pattern Recognition, June 2012, pp. 1098–1105
- [Yeganeh2013] H. Yeganeh and Z. Wang, "Objective quality assessment of tone-mapped images," Image Processing, IEEE Transactions on , vol. 22, no. 2, pp. 657-667, Feb 2013.
- [Zhang2011] L. Zhang, L. Zhang, X. Mou, and D. Zhang, "FSIM: A feature similarity index for image quality assessment," IEEE Transactions on Image Processing, vol. 20, no. 8, pp. 2378–2386, Aug 2011
- [Zhang2012] L. Zhang and H. Li, "SR-SIM: A fast and high performance IQA index based on spectral residual," in Proc. IEEE International Conference on Image Processing, Sept 2012, pp. 1473–1476
- [Zhang2013] Y. Zhang and D. M. Chandler, "No-reference image quality assessment based on log-derivative statistics of natural scenes,"Journal of Electronic Imaging, vol. 22, no. 4, 2013
- [Zhang2014] L. Zhang, Y. Shen, and H. Li, "VSI: A visual saliency-induced index for perceptual image quality assessment," IEEE Transactions on Image Processing, vol. 23, no. 10, pp. 4270–4281, Oct 2014

# Backup

# IQA in Synthetic Scenes

- Frame rendering in video games
  - Better real-time algorithms for photo-realistic images on powerful GPUs
  - More realistic lighting calculations
- Cloud gaming (e.g. Nvidia Grid servers)
- Livestreaming game play (e.g. YouTube Gaming)

# ESPL Database: Source Images

- 25 color images, 1920x1080 pixels in size
- Frames from video games
  - Multiplayer role playing games (such as War of Warcraft)
  - First person shooter games (such as Counter Strike)
  - Motorcycle and car racing games
- Frame from animated movies
  - The Lion King, Tinkerbell series, Avatar etc.



# ESPL Database: Source Content Parameters

- Spatial information (SI) indicates edge energy.

$$s_r = \sqrt{s_v^2 + s_h^2}$$

- $s_h$ and $s_v$: gray-scale images filtered with horizontal and vertical Sobel kernels respectively

$$SI = \sqrt{L/1080}\sqrt{\sum s_r^2 / P}$$

- P: Number of pixels in the filtered image
- L: Vertical resolution
- Colorfulness (CF) indicates variety and intensity of colors

$$CF = \sqrt{\sigma_{rg}^2 + \sigma_{by}^2} + 0.3\sqrt{\mu_{rg}^2 + \mu_{by}^2}$$

- Using opponent color spaces: $rg = R - G$ and $yb = 0.5(R+G) - B$

# ESPL Database: Source Complexity [Winkler2012]

- Spatial Information: Indicates edge energy
- Colorfulness: Indicates the variety and intensity of colors

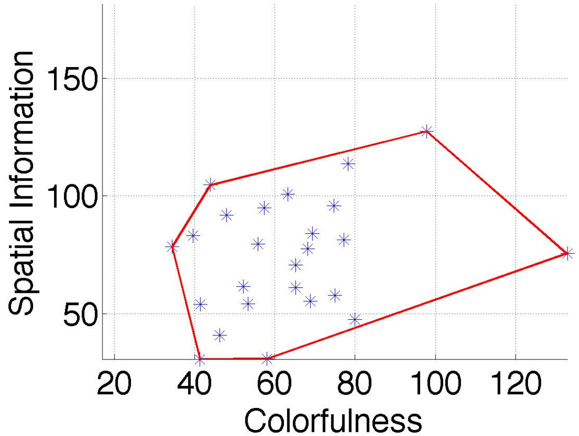


ESPL Database

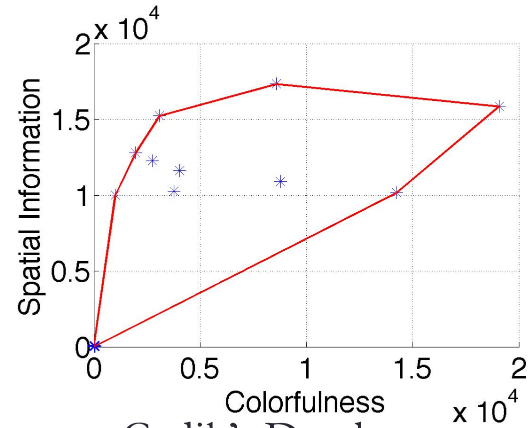


Cadik's Database

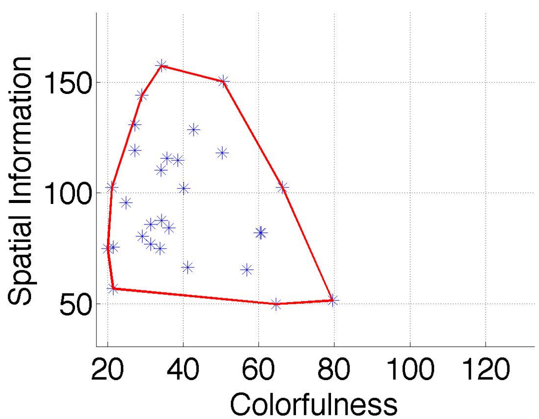


LIVE Database

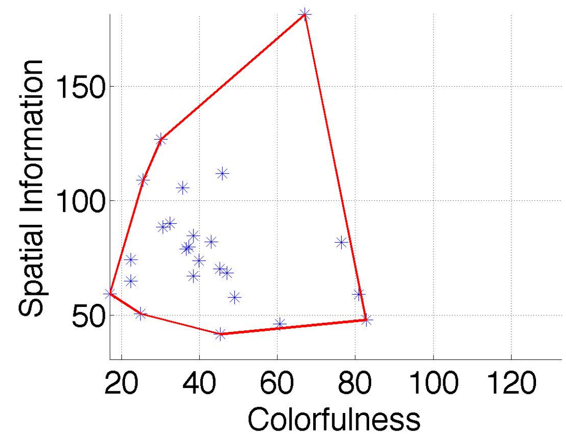


TID Database

Details

# ESPL Database: Processing of raw scores

- Raw scores were first converted to raw quality difference scores:

$$d_{ij} = r_{iref(j)} - r_{ij}$$

  - $r_{ij}$: Score assigned to $j$-th image by the $i$-th subject
  - $r_{iref(j)}$: Score assigned by same subject to corresponding reference
- Difference scores normalized for each subject and averaged

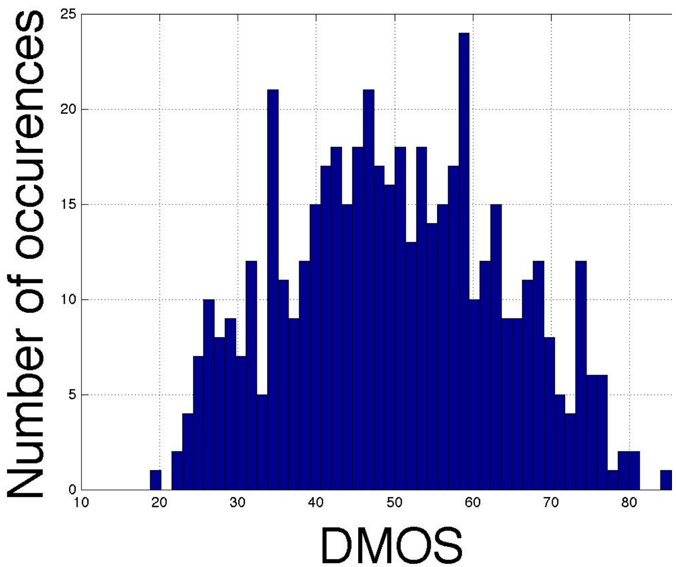


Histogram of DMOS scores

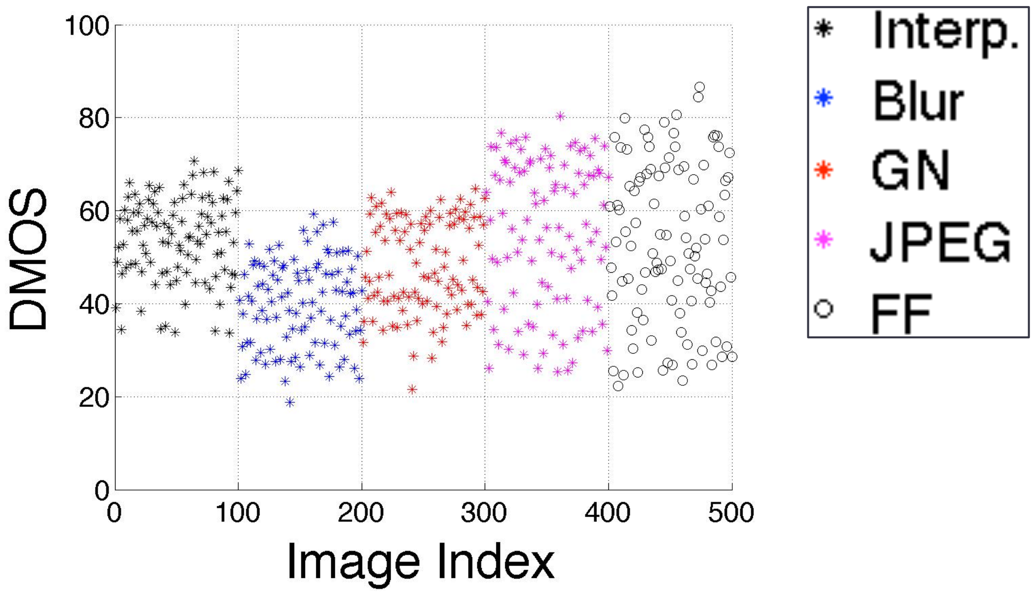


Scatter plot of DMOS scores

Back

# ESPL Database: Distortion Parameters

- Interpolation
  - Images downsampled by factors ranging from 3 to 6
  - Upsampled back using nearest neighbor interpolation
- Blur
  - RGB color channels filtered with circularly symmetric 2D Gaussian kernel
  - Standard deviation ranging from 1.25 to 3.5 pixels
  - Same kernel employed for each color channels
- Additive Noise:
  - Same noise variance used for all color channels
  - Noise standard deviation ranged from 0.071 to 0.316 pixels

Back

# ESPL Database: Distortion Parameters (cont'd)

- JPEG compression
  - MATLAB imwrite function was used
  - Bits per-pixel (bpp) ranged from 0.0445 to 0.1843.
  - Higher bpp images were not considered to better simulate playing a cloud video game under restricted bandwidth conditions.
- Simulated Fast Fading Channel
  - Original images compressed into JPEG2000 bitstreams
  - Wireless error resilience features enabled and 64 x 64 tiles
  - Transmitted over a simulated Rayleigh-fading channel
  - Signal-to-noise ratio (SNR) was varied at the receiver from 14 to 17 dB
  - SNRs greater than 17 dB did not introduce perceptible distortions due to the error resilience feature of the JPEG2000 codec.

Back

# ESPL Database: Methodology

- Single Stimulus Continuous Quality Scale (SSCQS) method
- Each subject evaluated each image
- Three sessions, of one hour each, separated by at least 24 hours.
  - Each session divided into two sub-sessions of 25 minutes
  - Separated by a break of five minutes.
- 64 subjects
  - Age range : 18 – 30 years
  - Mostly without prior experience in participation of subjective tests
- Verbal confirmation of 20/20 (corrected) vision was obtained
- Viewed roughly 175 test images during each session
  - Randomly ordered using a random number generator
- Testing sessions were preceded by training session of 10 images

# ESPL Database : Methodology (cont'd)

- User interface programmed on MATLAB using Psychology Toolbox
- NVIDIA Quadro NVS 285
- Dell 24 inches U2412M display
- 16:10 aspect ratio
- Normal office illumination
  - 540 lux measured with HS1010 digital light meter
- Each image displayed for 12 seconds
- Viewing distance: 2-2.25 times display height
- Scores between 0-100 was entered

# ESPL Database: Processing of raw scores

- Raw scores were first converted to raw quality difference scores:

$$d_{ijk} = r_{iref(j)k} - r_{ijk}$$

  - $r_{ijk}$: Score assigned to $j$-th image by the $i$-th subject in $k$-th session
  - $r_{iref(j)k}$: Score assigned by same subject to corresponding reference
- DMOS score is zero for reference images
- DMOS scores converted to Z-scores per session

$$\mu_{ik} = \frac{1}{N_{ik}} \sum_{j=1}^{N_{ik}} d_{ijk}$$

$$\sigma_{ik} = \sqrt{\frac{1}{N_{ik}-1} \sum_{j=1}^{N_{ik}} (d_{ijk} - \mu_{ik})^2}$$

$$z_{ijk} = \frac{d_{ijk} - \mu_{ik}}{\sigma_{ik}}$$

$$z'_{ij} = \frac{100(z_{ij}+3)}{6}$$

$$DMOS_j = \frac{1}{M} \sum_{i=1}^{M} z'_{ij}$$

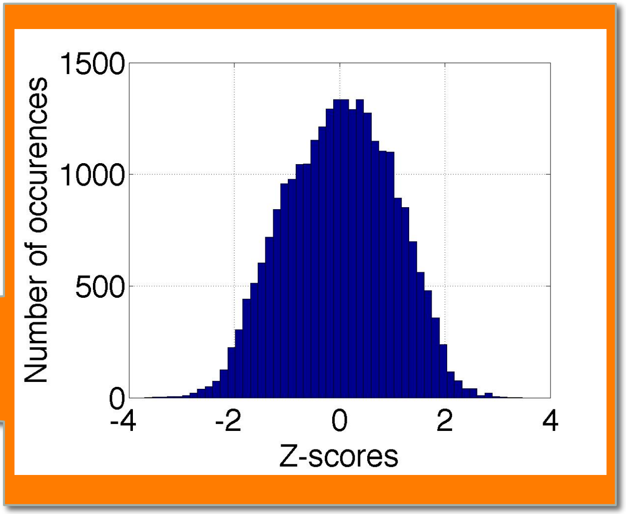


$N_{ik}$: Number of videos seen by $i$-th subject in $k$-th session

Back

# ESPL Database: Outlier rejection

- Done as per ITU-R BT 500.11 recommendation
- Compute kurtosis of scores per subject to check Gaussianity
- If kurtosis falls between the values of 2 and 4 (Gaussian)
  - Subject rejected if more than 5% of his scores falls outside $\pm 2\sigma$ from mean.
- For non Gaussian distributions
  - Subject rejected if more than 5% of his scores falls outside $\pm 4.47\sigma$ from mean.
- 12 out of 64 subjects rejected
- Testing degree of consensus among subjects:
  - Subjects divided into two groups randomly
  - DMOS scores for all the image calculated individually from each group
  - Pearson's linear correlation coefficient was 0.9813 between the groups
  - Shows a high level of consensus among the subjects

Back

# ESPL Database: Calculating correlations

- Let $Q_j$ be the quality predicted by the IQA algorithm for the j-th image.
- Four parameter monotonic logistic function fit IQA predictions to quality scores:

$$Q_j^{'} = \beta_2 + \frac{\beta_1 - \beta_2}{1 + \exp[-\frac{Q_j - \beta_3}{|\beta_4|}]}$$

- Spearman's Rank-order correlation coefficient: $SRCC = 1 - \frac{6\sum_{i=1}^{N} d_i^2}{N(N^2-1)}$
- where $d_i$ is the difference between the i-th image's ranks is subjective and objective evaluations.
- Kendall's correlation coefficient: $KCC = \frac{N_c - N_d}{0.5N(N-1)}$
- $N_c$ and $N_d$ are the number of concordant (of consistent rank order) and discordant (of inconsistent rank order) pairs in the data set respectively.

Back

# ESPL IQA: Scatter plot of DMOS vs IQA scores

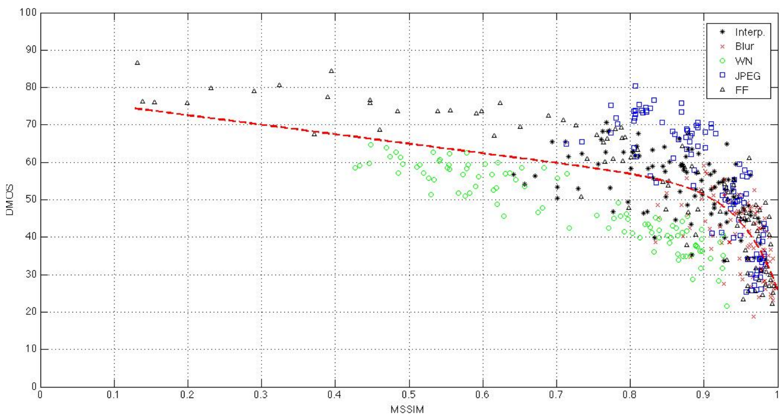


MSSIM

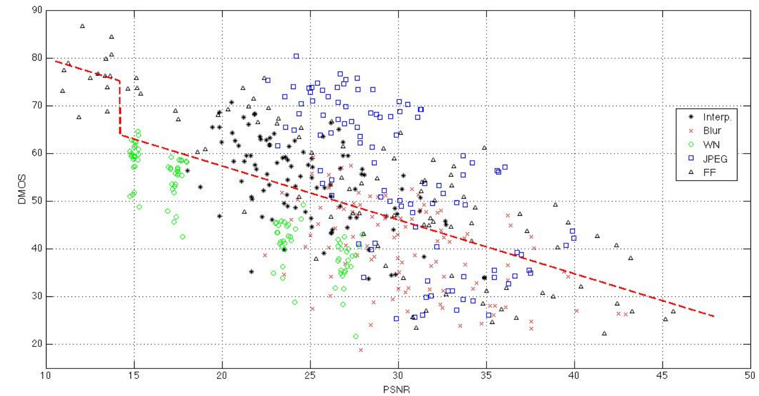


PSNR

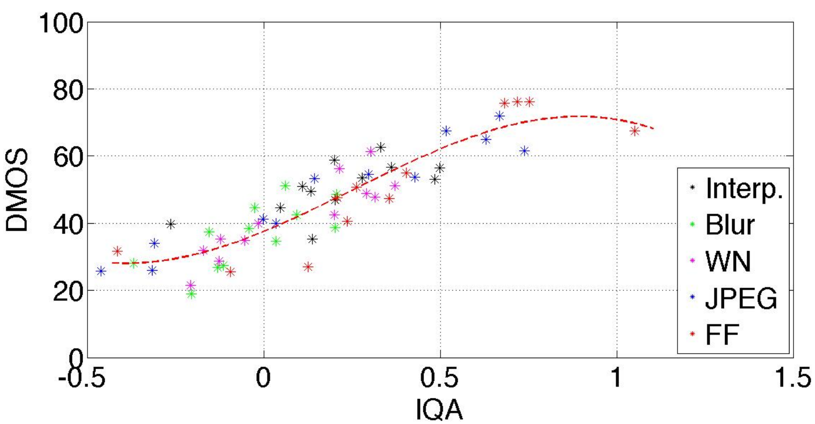


G-IQA-1

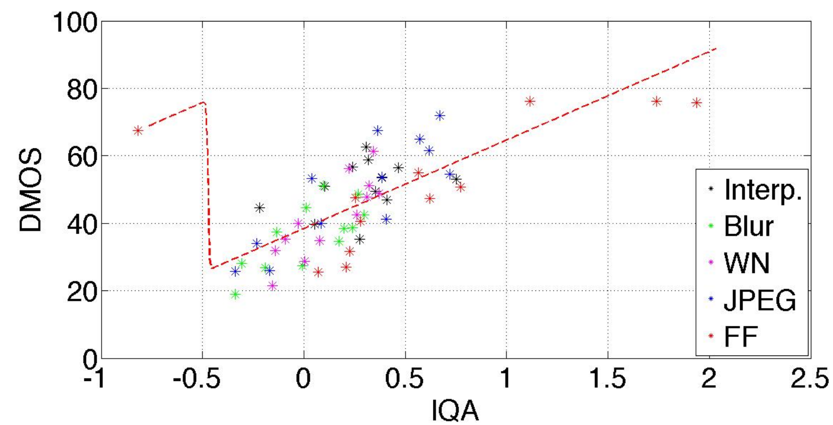


BRISQUE

# ESPL Objective IQA: Blur

- Blurred images led to a lower degree of correlation with human scores
- Lower degree of blur considered than natural images
- Some motion blur lead to aesthetically pleasing images [McGuire2012]
- Presence of blur may not always correspond to a lower subjective score

22 among 52 subjects rated the blurred version higher than the original one

Reference (DMOS = 0)

Blurred (5x5 Gaussian kernel. $\sigma$ = 1.25 pixels) (DMOS = 18.86)

Back

# ESPL Objective IQA: Interpolation

- Lowest degree of correlation with human scores among all distortions
- Most Apparent Distortion measure achieves highest correlation
- It advocates multiple strategies for determining overall image quality
  - Based on whether the distortions are near-threshold or supra-threshold
- Low downsampling factors result in near-threshold artifacts
  - Almost imperceptible at normal viewing distances
- Higher downsampling factors result in supra-threshold artifacts

Reference (DMOS = 0)

Interpolated (DMOS = 56.40)

Back

# ESPL Objective IQA: Role of Pooling

- Efficient pooling strategies play an important role
- Visual Saliency Index, Spectral Residual based Similarity Measure
  - Use visual fixations based pooling strategies
- Gradient Magnitude Similarity Index
  - Use standard deviation of gradient map
- Using visual fixations in synthetic scenes is promising direction

Reference

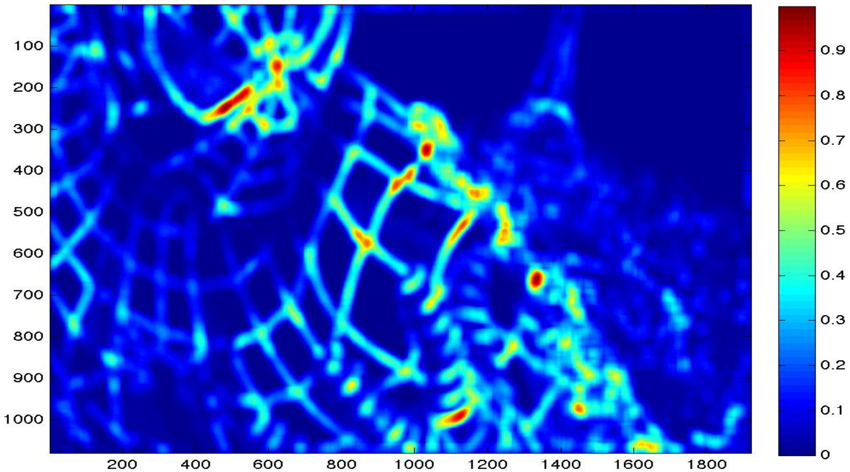


Spectral Residual Saliency

Back

# ESPL Objective IQA: MSCN Images

Original Image

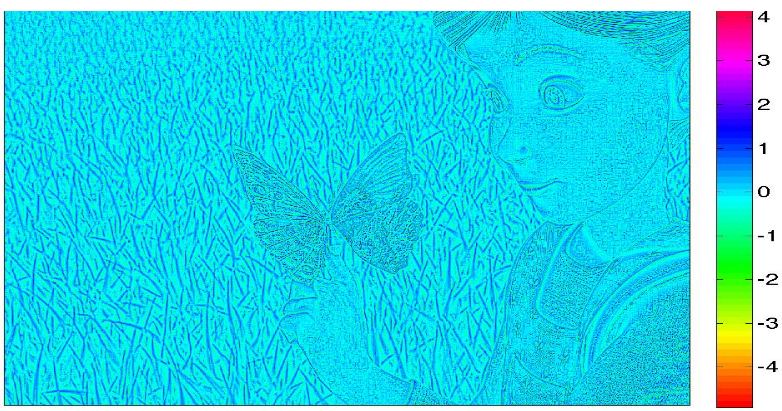


MSCN Image

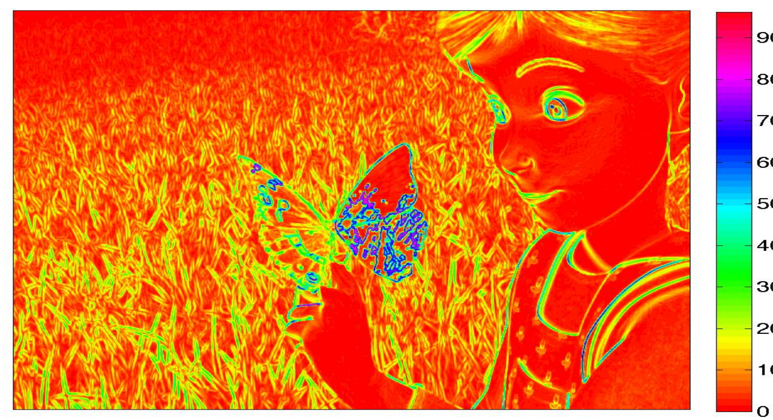


Standard Deviation Image

# ESPL Objective IQA : Modeling MSCN Pixels

- MSCN coefficients modeled by the following distributions:
  - Generalized Gaussian (GGD)
  - Symmetric Alpha Stable (SaS): For highly kurtotic empirical histograms

Mean square error, J-Divergence, and Pearson's Chi-squared values for distributions fitted to histograms of MSCN coefficients, averaged over 221 pristine synthetic images [Kundu 2014]

Chi-Squared value at 99% confidence interval = 6.635

| | MSE | J | Chi Square |
|---|---|---|---|
| GGD | 0.00257 | 0.0772 | 0.00252 |
| SAS | 0.00264 | 0.0948 | 0.00174 |


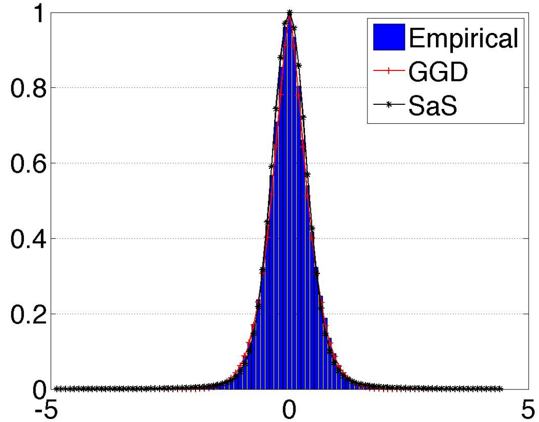


Back

# ESPL IQA: Modeling of MSCN Gradients

- Distribution of the gradient magnitude of MSCN coefficients
  - Modeled using Rayleigh, Weibull and Nakagami distributions

Mean square error, J-Divergence, and Pearson's Chi-squared values for distributions fitted to histograms of MSCN coefficients, averaged over 221 pristine synthetic images [Kundu 2014]

| | MSE | J | Chi Square |
|---|---|---|---|
| Rayleigh | 0.00891 | 4.730 | 0.769 |
| Weibill | 0.0251 | 5.00432 | 0.663 |
| Nakagami | 0.00916 | 5.304 | 0.892 |


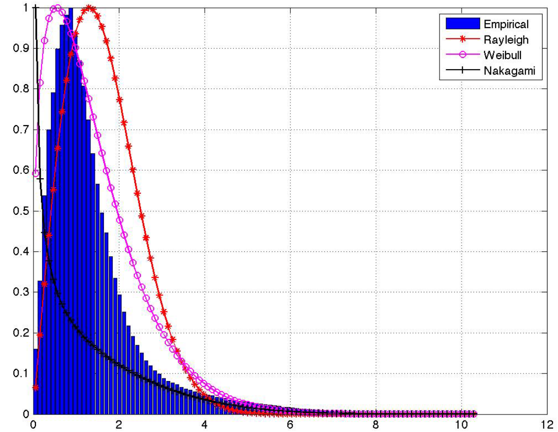


Back

# Generalized Gaussian Density

- The **GGD** $p_g(r) = \frac{\beta}{2\sigma\Gamma\left(\beta^{-1}\right)} \exp\left(\left|r\right|/\sigma\right)^{\beta} \quad r \in \Re, \sigma, \beta > 0$

  includes the **special cases**

  $\beta = 1$ (**laplacian** density)

  $\beta = 2$ (**gaussian** density)

  $\beta = \infty$ (**uniform** density)

- Many authors have observed the **GGD behavior** of **BP image** signals.
  - Wavelet coefficients
  - DCT coefficients

[Ref: Dr. Alan C. Bovik, EE381V Digital Video, Spring 2015]

  - **Usually** reported that b » 1 but **varies** (0.8 < b < 1.4).

# Symmetric Alpha Stable

- A random variable X is called stable if its characteristic function can be expressed as:

$$\varphi(t;\alpha,\beta,c,\mu) = \exp\left[\, it\mu - |ct|^{\alpha}\left(1 - i\beta\,\mathrm{sgn}(t)\Phi\right)\,\right]$$

- sgn(t): sign of t

$$\Phi = \tan(\pi\alpha/2)$$

-

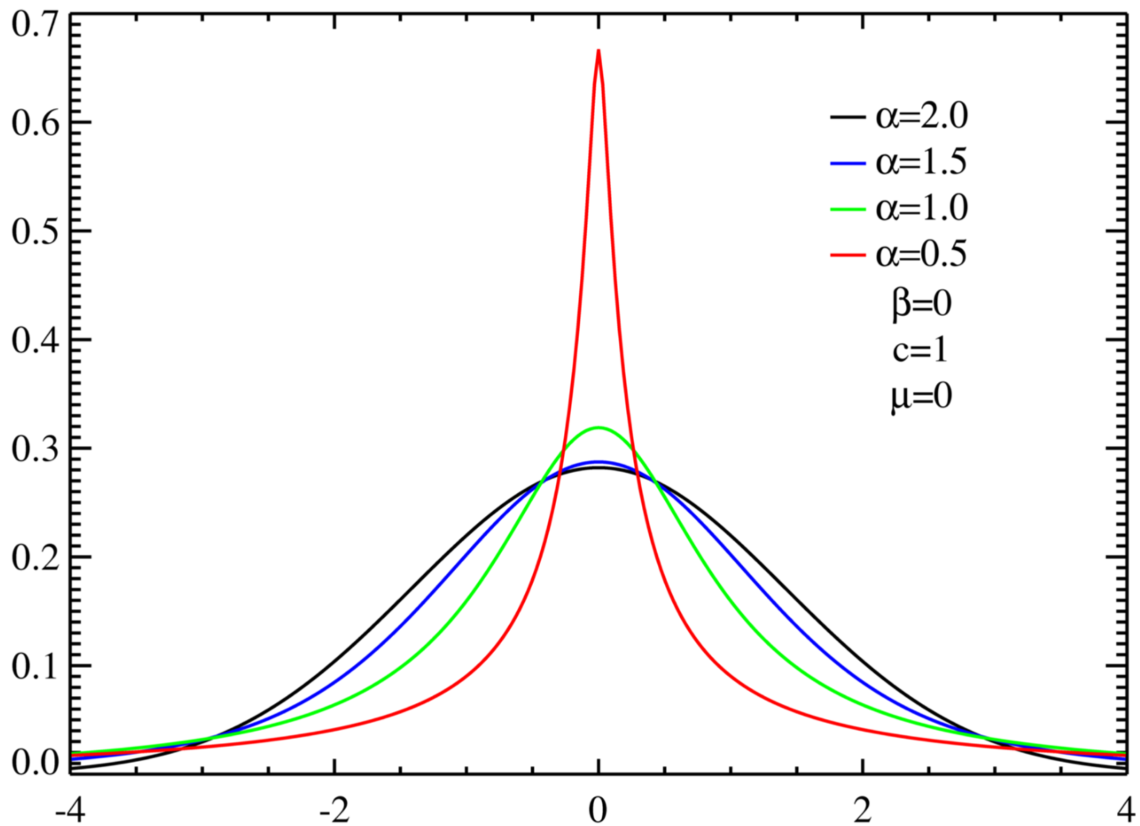

# Steerable Filter

- Create **directional derivative** of **gaussian** in **arbitary direction** by a **coordinate rotation** by **q**:

$$h_\theta(\mathbf{x}) = \frac{-1}{2\pi\sigma^4}\left[(\cos\theta)x + (\sin\theta)y\right]\exp\left[\frac{-\left(x^2+y^2\right)}{2\sigma^2}\right]$$

$$\overset{\mathcal{F}}{\longleftrightarrow}\quad j\cdot\left[(\cos\theta)U + (\sin\theta)V\right]\cdot\exp\left[-2(\pi\sigma)^2\left(U^2+V^2\right)\right]$$

- In particular:

$$h_\theta(\mathbf{x}) = (\cos\theta)h_0(\mathbf{x}) + (\sin\theta)h_{\frac{\pi}{2}}(\mathbf{x}) \quad \overset{\mathcal{F}}{\longleftrightarrow} \quad (\cos\theta)H_0(\mathbf{u}) + (\sin\theta)H_{\frac{\pi}{2}}(\mathbf{u}) = H_\theta(\mathbf{u})$$

- A **derivative-of-gaussian** filter of **any orientation** (derivative direction ) is exactly a **linear combination of two** orthogonal derivative-of-gaussian filters

[Ref: Dr. Alan C. Bovik, EE381V Digital Video, Spring 2015]

# ESPL IQA: Steerable Pyramid comparison

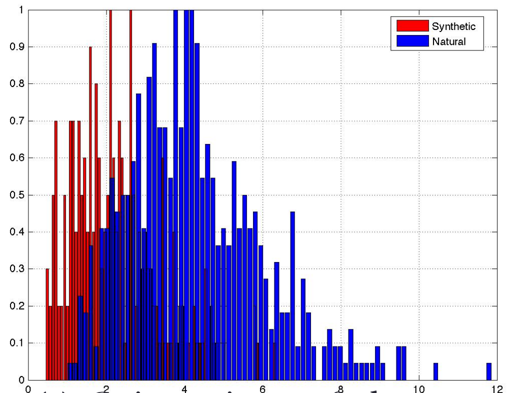


(a) Orientation = 0 degree

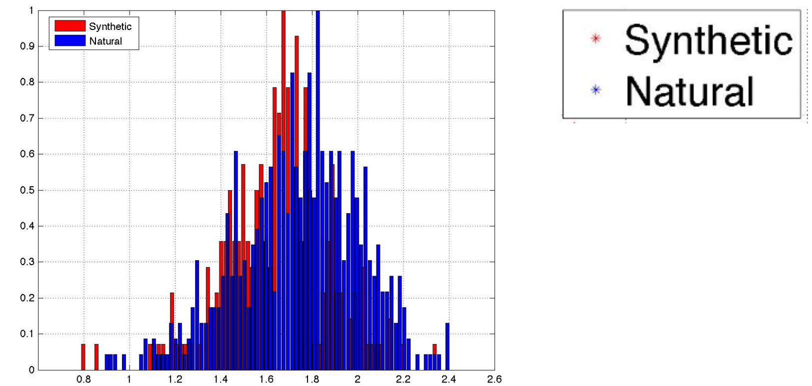


(c) Orientation = 0 degree

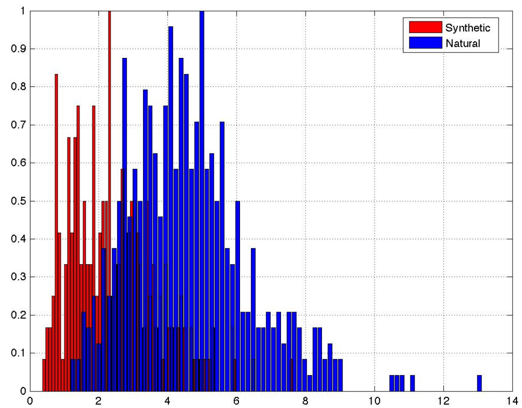


(b) Orientation = 60 degrees

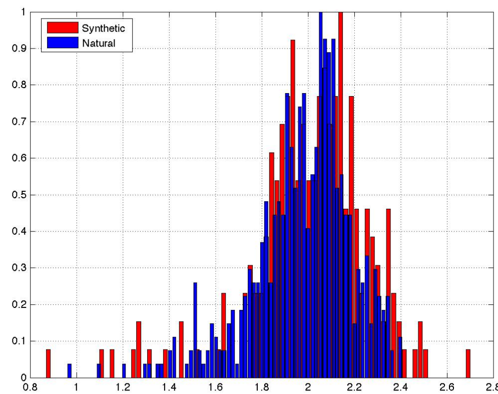


(d) Orientation = 60 degrees

Histogram of scale (a)(b) and shape parameters(c)(d) of the steerable pyramid decomposition of synthetic images (221 images) and natural images [Martin2001] (500 images from Berkeley Segmentation Dataset)

# ESPL IQA: Comparison with Natural Scenes

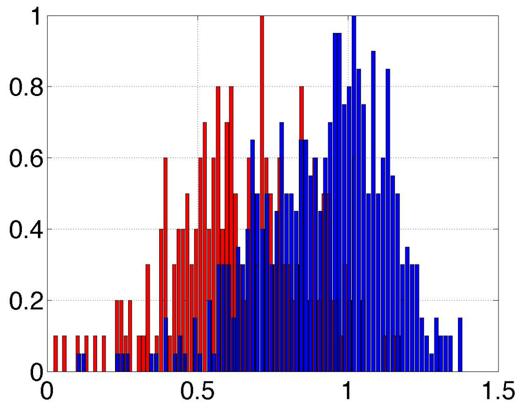


Histogram of scale parameter
(JS divergence = 1.5655)

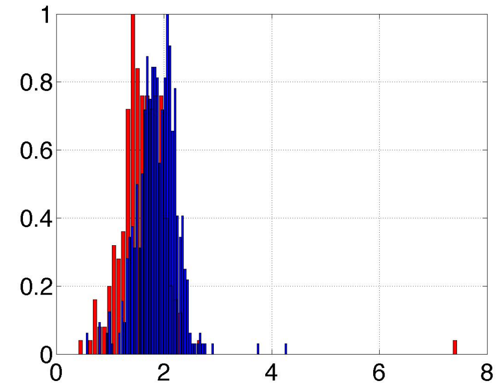


Histogram of shape parameter
(JS divergence = 1.0503)

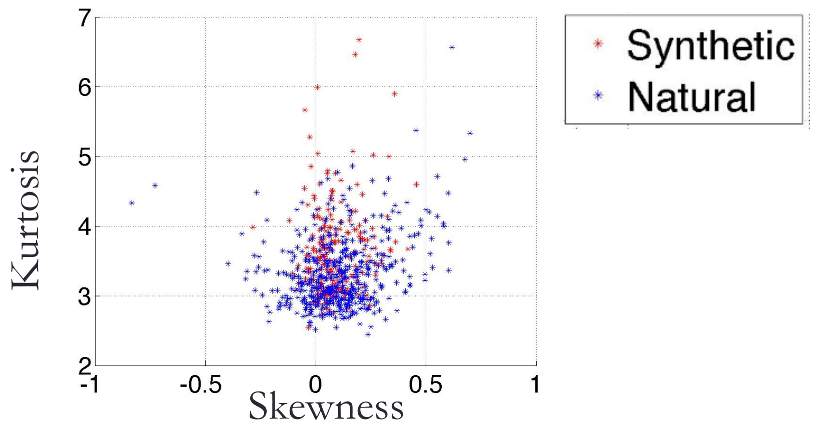


Skewness-kurtosis scatter plot
of MSCN coefficients of synthetic images[Kundu2014] (221 images) and natural images [Martin2001] (500 images from Berkeley Segmentation Dataset)

# ESPL IQA: Distorted Image Statistics in Different Domains

- Different distortions affect scene statistics characteristically
- Can be used for distortion classification and blind quality prediction

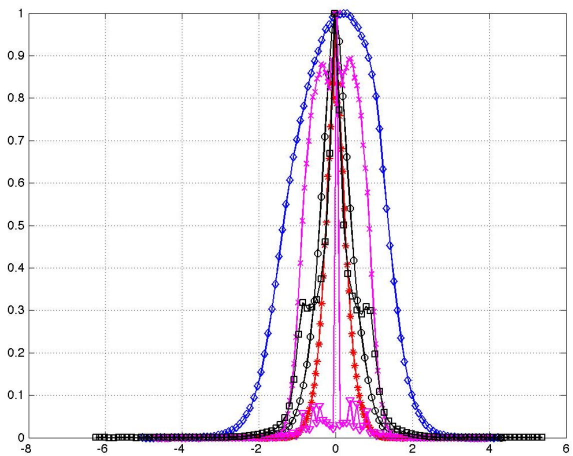

MSCN Coefficients

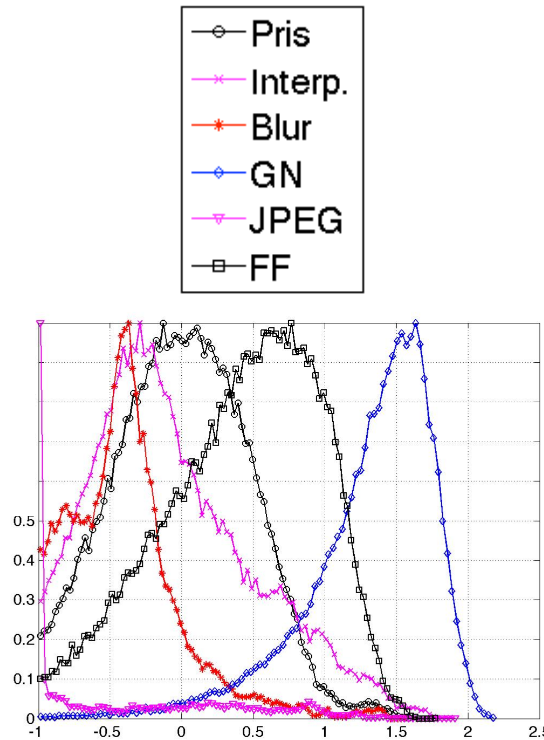


Curvelet Coefficients

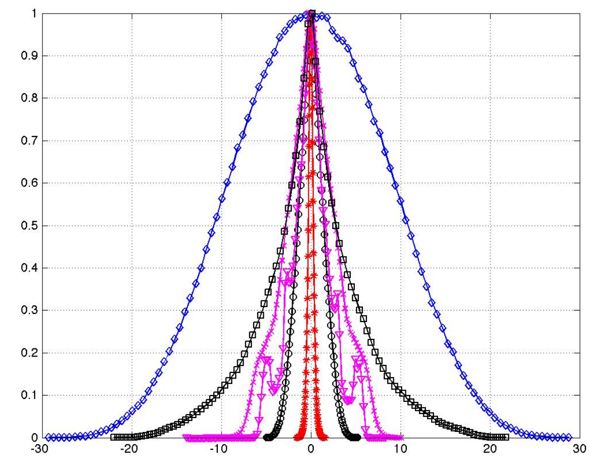

Steerable Pyramid Wavelet Coefficients

Back

# ESPL Objective IQA: Classification using NSS

- Singular value decomposition of blind IQA features in 2-D

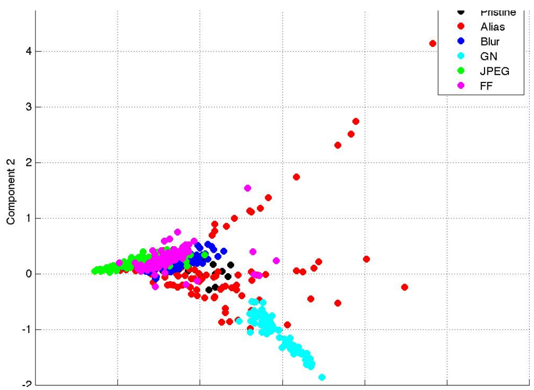


BRISQUE features (MSCN)

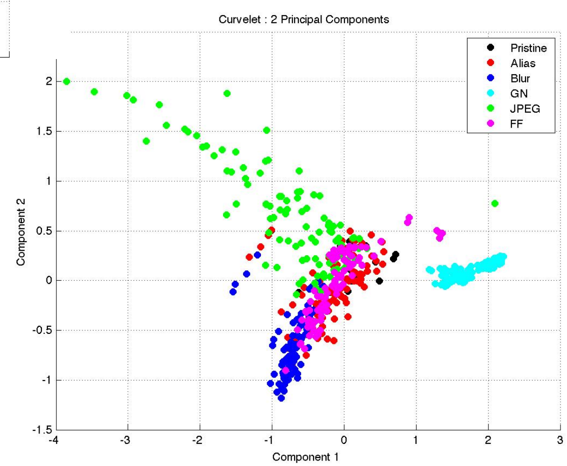


CurveletQA features (Curvelets)

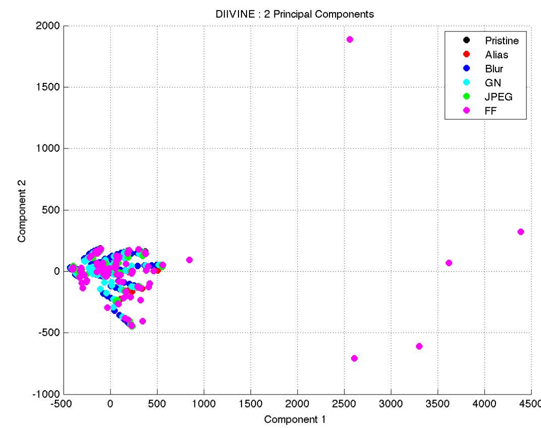


DIIVINE features (Wavelets)

[Back](#)

# ESPL IQA : Box plot of No-reference SROCC

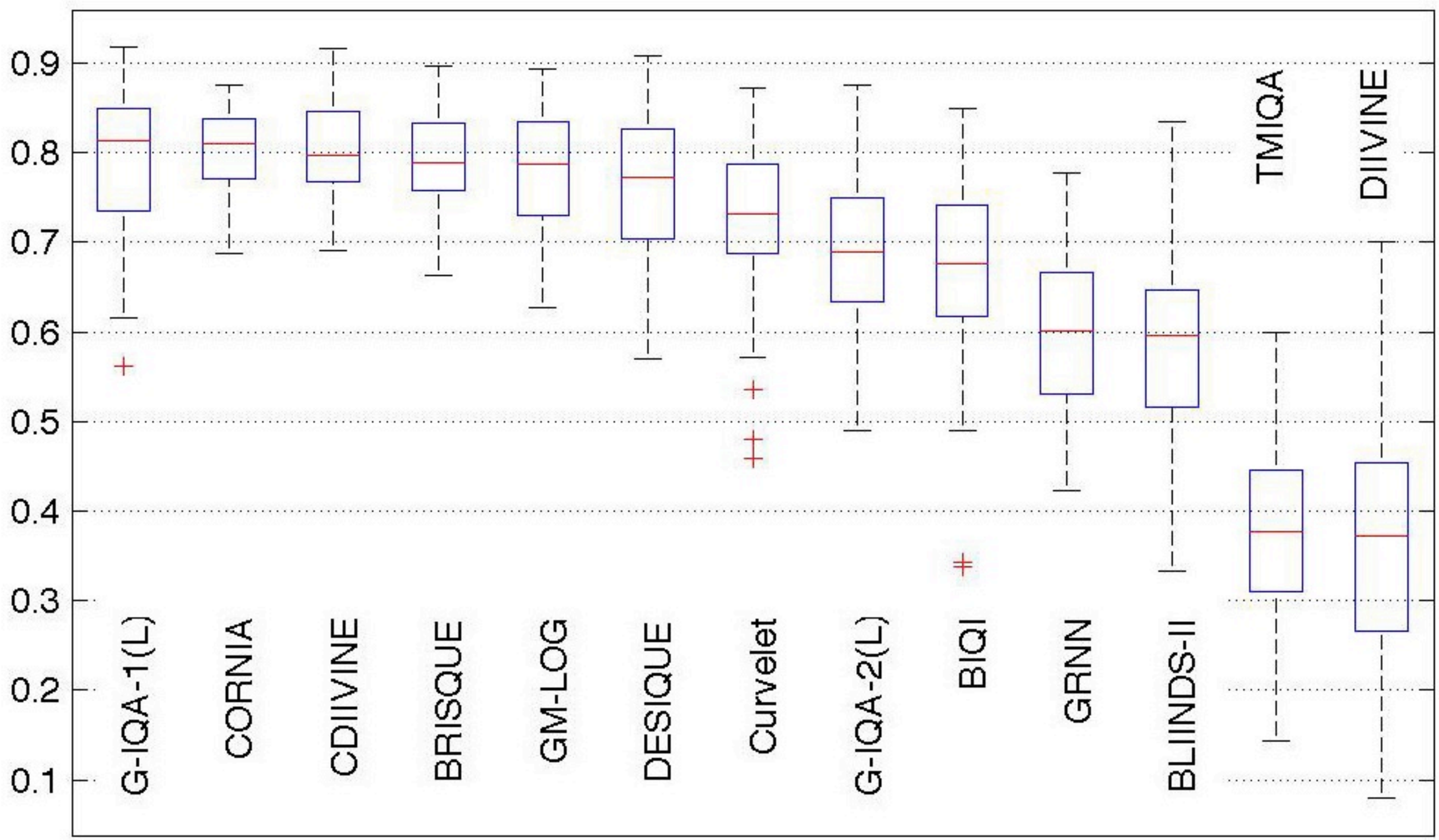


Back

# ESPL IQA: Performance-Time Complexity Tradeoff (FR, RR-IQAs)

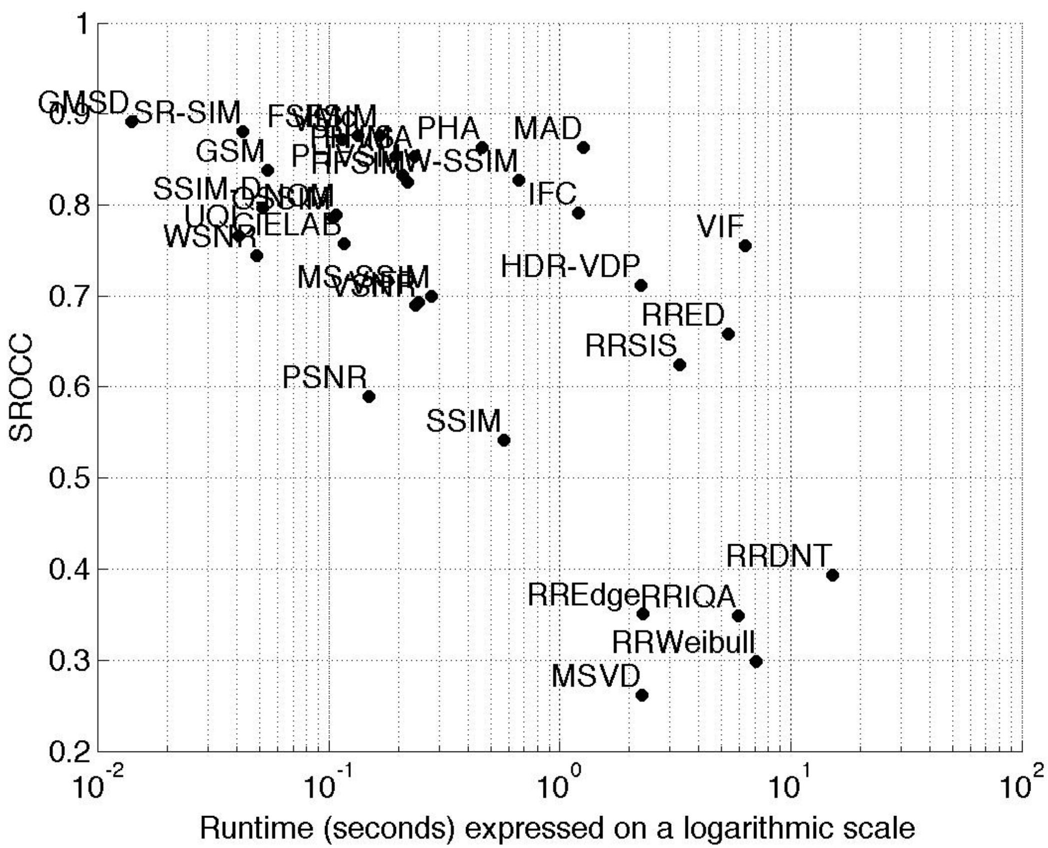


- FR-IQA: SR-SIM, GMSD show good performance-complexity tradeoff

# ESPL IQA: Performance-Time Complexity Tradeoff (NR-IQAs)

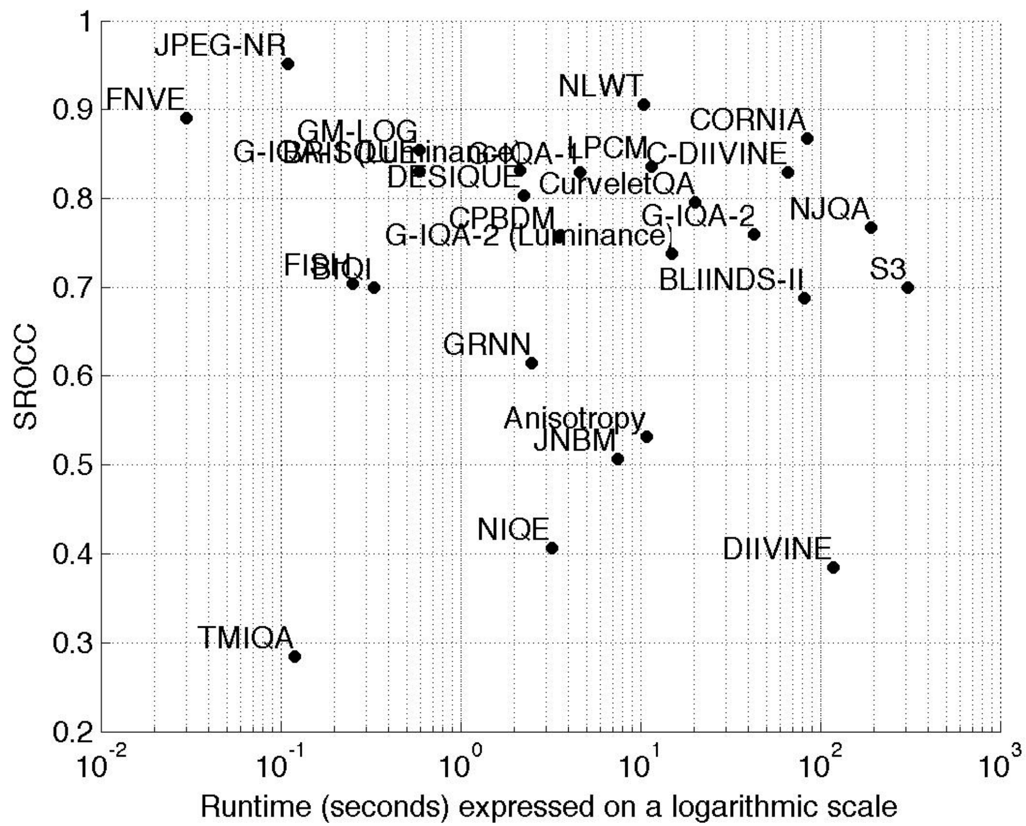


- Some NR-IQA metrics comparable with the best FR-IQA algorithms.

# HDR IQA: Multi Exposure Fusion

$$Y(i) = \sum_{k-1}^{K} W_k(i) X_k(i)$$

- $K$ : Number of multi-exposure input images
- $Y$ : Fused Image
- $X_k(i)$ : Luminance (or coefficient amplitude in transform domain) at $i$-th pixel in $k$-th exposure image
- $W_k(i)$ : Weight at $i$-th pixel in $k$-th exposure image
  - Spatially adaptive
  - Varies according to perceptual importance of different exposure levels.
- Requires
  - Camera calibration
  - Motion compensation

Back

# HDR IQA: Tone Mapped Quality Index (TMQI)

[Yeganeh, 2013]

- Based on Structural Similarity (SSIM) Index
- Does not penalize change in signal strength between HDR and SDR image patches
- Only penalized cases when signal strength is significant in one image patch but not in the other
- Local standard deviation nonlinearly mapped so that:
  - Significant signal strength mapped to 1
  - Insignificant signal strength mapped to 0
- CDF of Gaussian distribution is used for non-linear mapping:

$$p(s) = \frac{1}{\sqrt{2\pi}\theta_s} \int_{-\infty}^{s} \exp\left[-\frac{(x-\tau_s)^2}{2\theta_s^2}\right] dx$$

- Structural fidelity computation over multiple scales

Back

# HDR IQA: Naturalness Measure

- TMQI combines structural similarity score (S) with naturalness (N) measure

$$Q = aS^{\gamma} + (1-a)N^{\delta}$$

$$N = \frac{1}{K} P_m P_d$$

- $P_m$: Gaussian fit to means of natural images $P_m(m) = \frac{1}{\sqrt{2\pi}\sigma_m} \exp\left[-\frac{m-\mu_m}{2\sigma_m^2}\right]$

- $P_d$: Beta fit to standard deviations of natural images:

$$P_d(d) = \frac{(1-d)^{\beta_d - 1} d^{\alpha_d - 1}}{\mathrm{B}(\alpha_d, \beta_d)}$$

- $\gamma, \delta$ are sensitivity parameters

Back

# HDR IQA: Itti and Koch's Saliency

Back

- Different scales: Implemented as Gaussian Pyramid
- Center Surround mechanism:
  - Implemented with DoG
- LPF repeated over multiple scales
- 3 scales, 4 orientations used

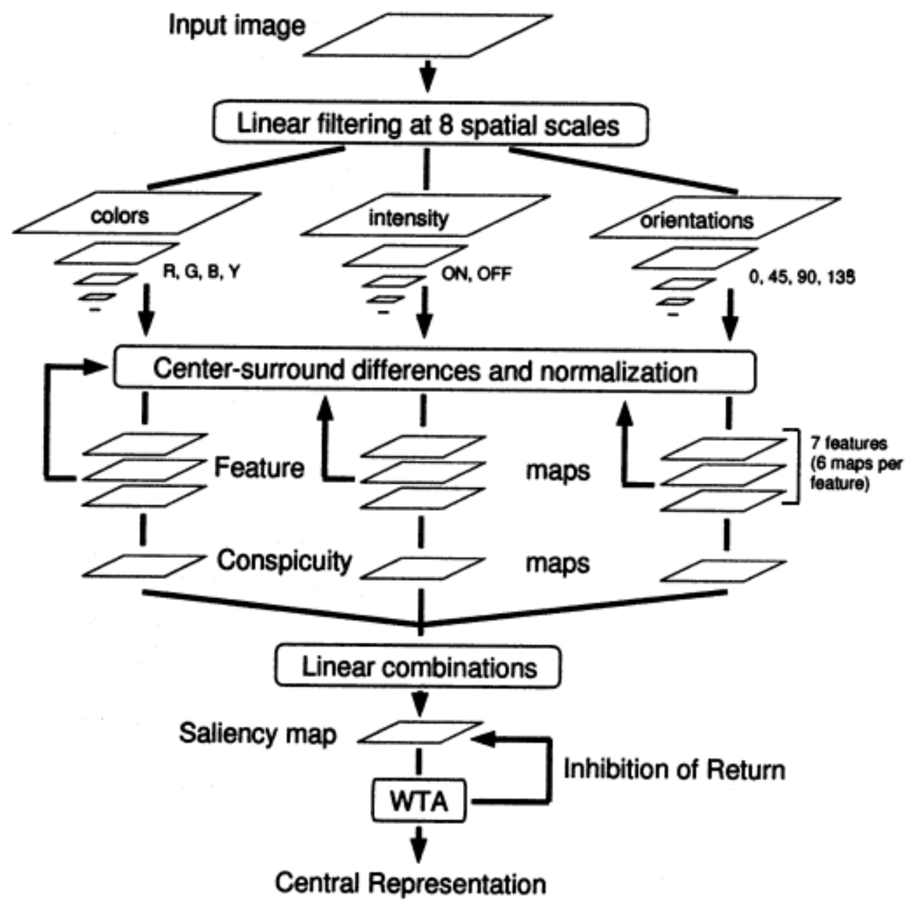


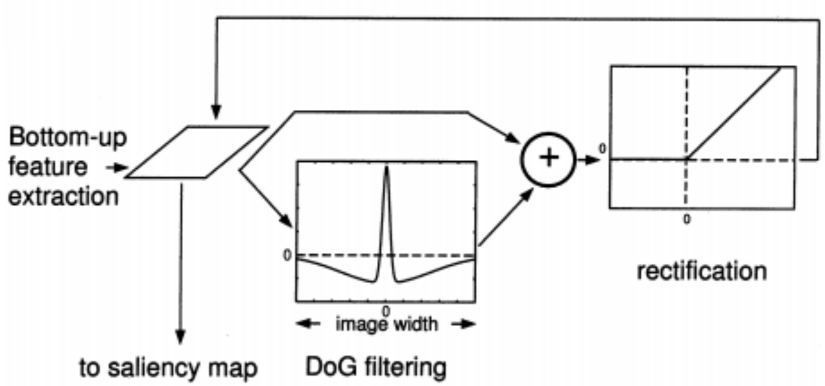

Back

# HDR IQA: Local weighing using local entropy

- Local entropy filtering at every pixel leads to detecting high contrast regions
- Gives a measure of local randomness

$$H(I) = -\sum_i p(h_i)\log[p(h_i)]$$

  - $p(h)$ is the probability of intensity $h$

Tone mapped image

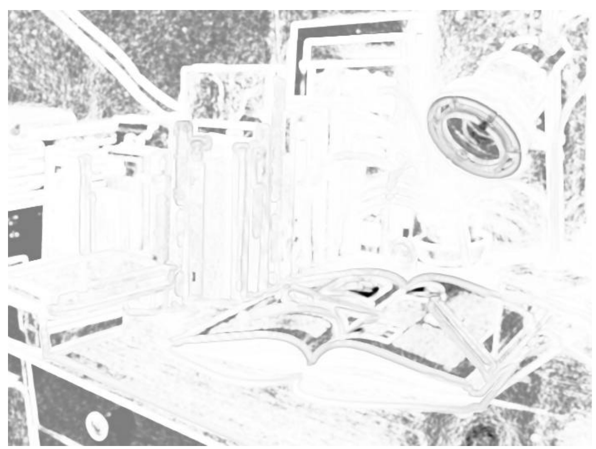

Structural fidelity map

Structural fidelity with pooling

# HDR IQA: Results on HDR-JPEG database [Narwaria2013]

- 10 source HDR images
- Each source image has 14 degraded versions
- JPEG coding with 7 different bit rates.
- SSIM and MSE are two optimization criteria used

Back

| FR-IQA Algorithms | SROCC | PLCC | Time(s) |
|---|---|---|---|
| SHDR-TMQI (Proposed) | 0.8510 | 0.8533 | 3.0003 |
| TMQI-NSS-Sigma (Proposed) | 0.8485 | 0.8520 | 1.6470 |
| TMQI-NSS-Entropy (Proposed) | 0.8454 | 0.8645 | 6.7424 |
| Tone Mapped Image Quality Index (TMQI)[Yeganeh2013] | 0.7947 | 0.8057 | 3.4394 |
| FSITM-TMQI[Nafchi2014] | 0.6300 | 0.6584 | 8.3486 |
| TMQI-II[Ma2015] | 0.5096 | 0.5137 | 1.3424 |
| Feature Similarity Index for Tone-Mapped Images(FSITM) [Nafchi2014] | 0.4720 | 0.5167 | 5.2617 |
| STMQI[Nasrinpour2015] | 0.3464 | 0.3244 | 11.9965 |

# ESPL-LIVE HDR Database: Source Complexity

- Spatial Information: Indicates edge energy
- Colorfulness: Indicates the variety and intensity of colors
- Computed on medium exposure image in source exposure stack

Back

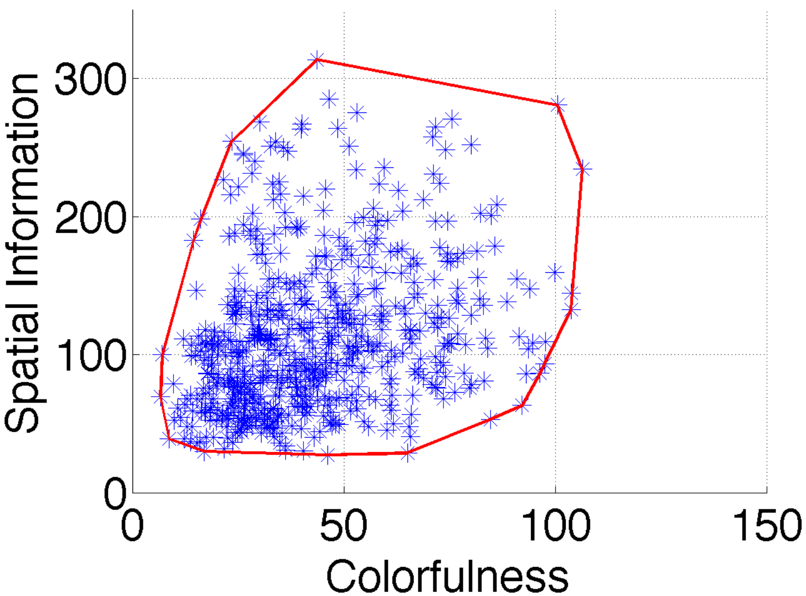


ESPL-LIVE HDR Database

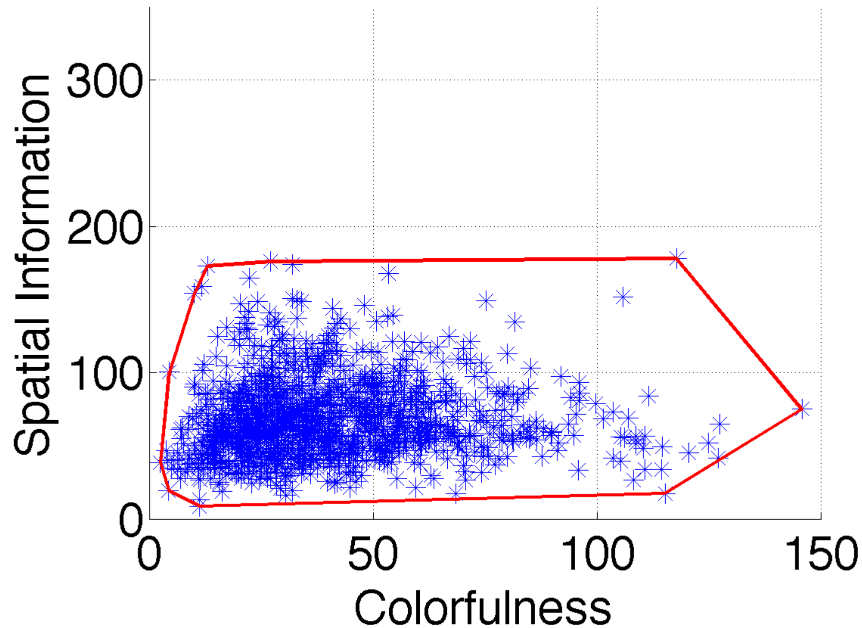


LIVE Challenge Database[Ghadiyaram2016]

Details

# HDR-IQA: Z-Scores Distributions

Back

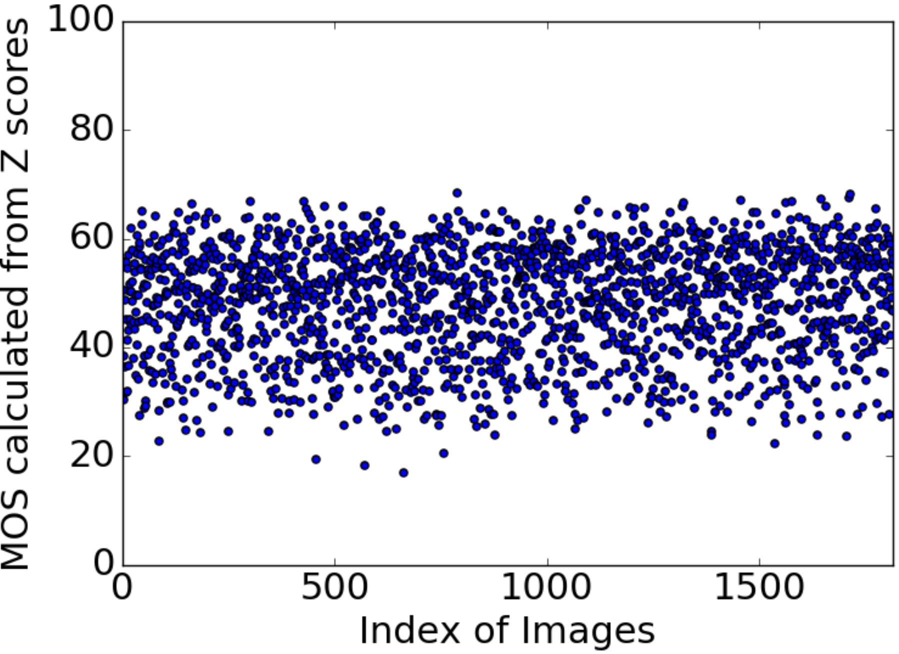


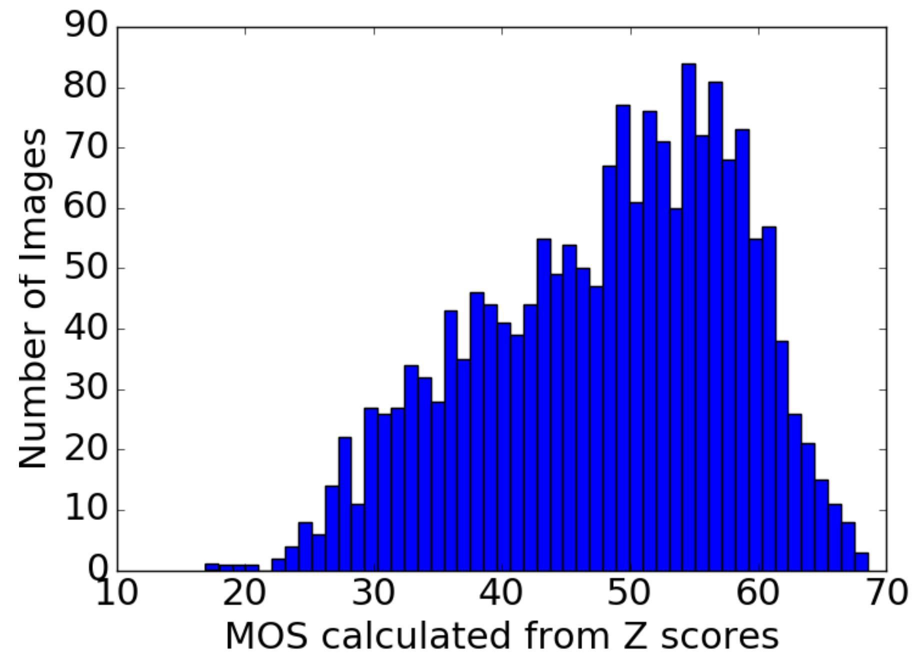

# Gradient Image Quality Assessment-1

Back

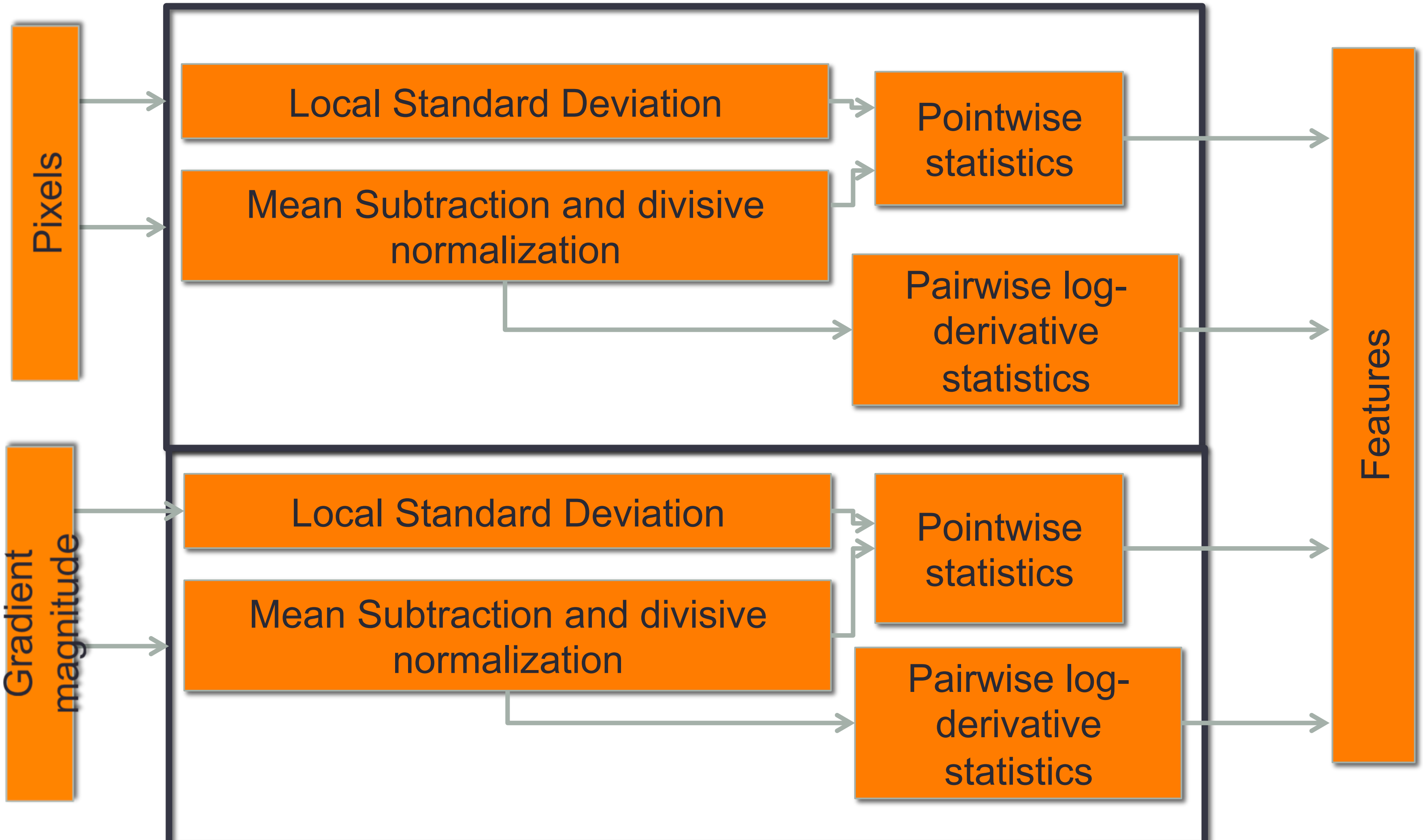

# Gradient Image Quality Assessment-2

[Back](#)

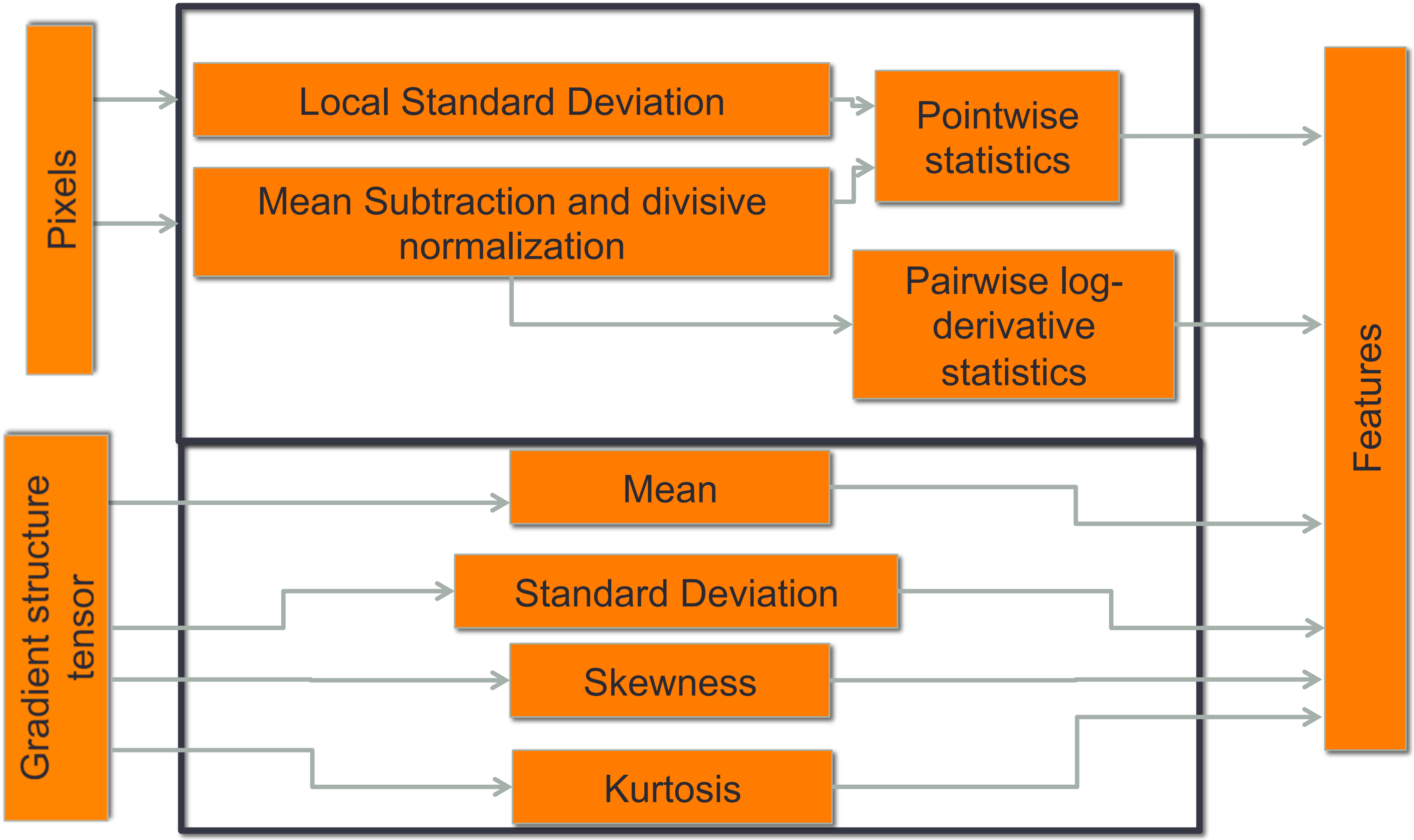

# HDR IQA: Log Derivative Computation

Back

- Logarithm of each MSCN coefficient is computed

$$\hat{I}(i,j) = \frac{I(i,j) - \mu(i,j)}{\sigma(i,j) + 1}$$

$$J(i,j) = \log[\hat{I}(i,j) + K]$$

- Seven types of log-derivatives defined

$$D1: \nabla_x J(i,j) = J(i,j+1) - J(i,j)$$

$$D2: \nabla_y J(i,j) = J(i+1,j) - J(i,j)$$

$$D3: \nabla_{xy} J(i,j) = J(i+1,j+1) - J(i,j)$$

$$D4: \nabla_{yx} J(i,j) = J(i+1,j-1) - J(i,j)$$

$$D5: \nabla_x \nabla_y = J(i-1,j) + J(i+1,j) - J(i,j-1) - J(i,j+1)$$

$$D6: \nabla_{cx} \nabla_{cy} J(i,j)_1 = J(i,j) + J(i+1,j+1) - J(i,j+1) - J(i+1,j)$$

$$D7: \nabla_{cx} \nabla_{cy} J(i,j)_2 = J(i-1,j-1) + J(i+1,j+1) - J(i-1,j+1) - J(i+1,j-1)$$

# Gradient Structure Tensor Coherence

Back

- $G_x$ : Vertical component of gradient
- $G_y$: Horizontal component of gradient
- Computed by convolving with difference-of-Gaussians
- Gradient structure tensor is defined as:

$$J = \begin{bmatrix} f(G_x) & f(G_x G_y) \\ f(G_x G_y) & f(G_y) \end{bmatrix}$$

$$f(V) = \sum_{l,k} w[i,j] V(i-k, j-k)^2$$

- $\lambda_1$ and $\lambda_2$ are the two eigenvalues of gradient structure tensor
- C: Gradient structure tensor coherence:

$$C = \left( \frac{\lambda_1 - \lambda_2}{\lambda_1 + \lambda_2} \right)^2$$

- Computed over 9x9 non-overlapping blocks
- Features are: mean, standard deviation, skewness and kurtosis of C

# No-reference IQAs on LIVE Database

Back

| Algorithms | JP2K | JPEG | GN | Blur | FF | Overall |
|---|---|---|---|---|---|---|
| GM-LOG | 0.882 | 0.878 | 0.978 | 0.915 | **0.899** | **0.914** |
| G-IQA-1 | **0.905** | **0.883** | 0.983 | 0.917 | 0.836 | 0.906 |
| G-IQA-2 | 0.904 | 0.867 | **0.982** | 0.920 | 0.841 | 0.904 |
| BRISQUE | 0.878 | 0.852 | 0.962 | **0.941** | 0.863 | 0.902 |
| BLIINDS-II | 0.907 | 0.846 | 0.939 | 0.906 | 0.884 | 0.897 |
| DESIQUE | 0.875 | 0.824 | 0.975 | 0.908 | 0.829 | 0.878 |
| CurveletQA | 0.816 | 0.827 | 0.969 | 0.896 | 0.826 | 0.863 |
| DIIVINE | 0.824 | 0.759 | 0.937 | 0.854 | 0.759 | 0.827 |
| *MS-SSIM* | *0.963* | *0.979* | *0.977* | *0.954* | *0.939* | *0.954* |
| *SSIM* | *0.939* | *0.947* | *0.964* | *0.905* | *0.939* | *0.913* |
| *PSNR* | *0.865* | *0.883* | *0.941* | *0.752* | *0.874* | *0.864* |

Italics indicate full-reference algorithms

# F-test on residuals between IQAs and DMOS

Back

| | A | B | C | D | E | F | G | H | I |
|---|---|---|---|---|---|---|---|---|---|
| A | ---- | ---- | 1--1 | 1--1 | 1--1 | 1--1 | 1--1 | 1-11 | ---1 |
| B | ---- | ---- | 1--1 | 1--1 | 1--1 | 1--1 | 1--1 | 11-1 | 1--1 |
| C | 0--0 | 0--0 | ---- | ---- | ---- | ---- | ---- | ---- | 0--- |
| D | 0--0 | 0--0 | ---- | ---- | ---- | ---- | ---- | ---- | 0--- |
| E | 0--0 | 0--0 | ---- | ---- | ---- | ---- | ---- | ---- | ---- |
| F | 0--0 | 0--0 | ---- | ---- | ---- | ---- | ---- | ---- | 0--- |
| G | 0--0 | 0--0 | ---- | ---- | ---- | ---- | ---- | ---- | ---- |
| H | 0-00 | 00-0 | ---- | ---- | ---- | ---- | ---- | ---- | 0--0 |
| I | ---0 | 0--0 | 1--- | 1--- | ---- | 1--- | ---- | 1--1 | ---- |

A : G-IQA-1, B : G-IQA-2, C : DESIQUE, D : BRISQUE. E : GM-LOG
F : C-DIIVINE, G : DIIVINE, H : BLIINDS-II, I : CurveletQA

# HDR-IQA: Box plot of No-reference SROCC

Back

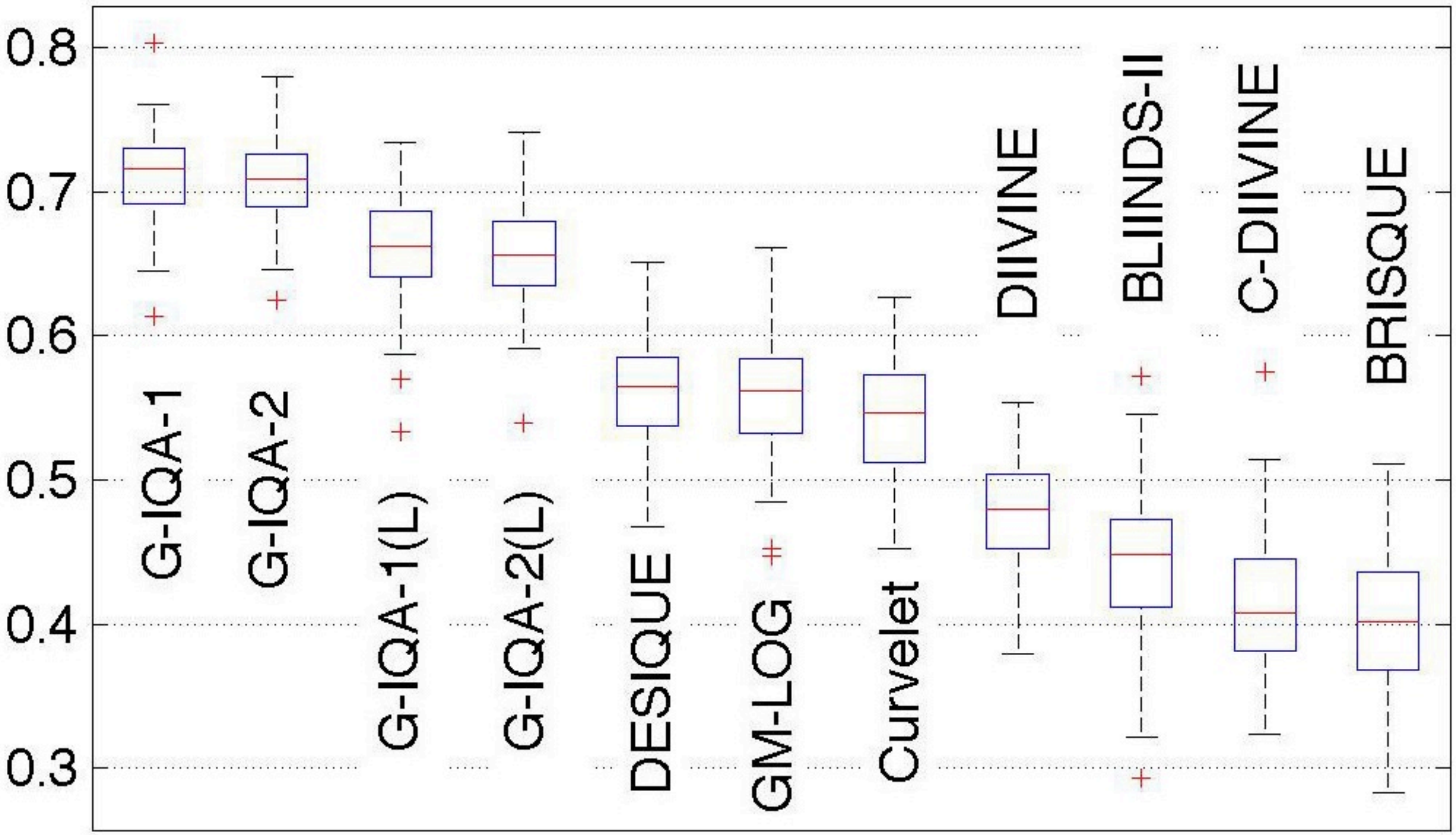

# HDR IQA: Scatter plot of MOS vs IQA scores

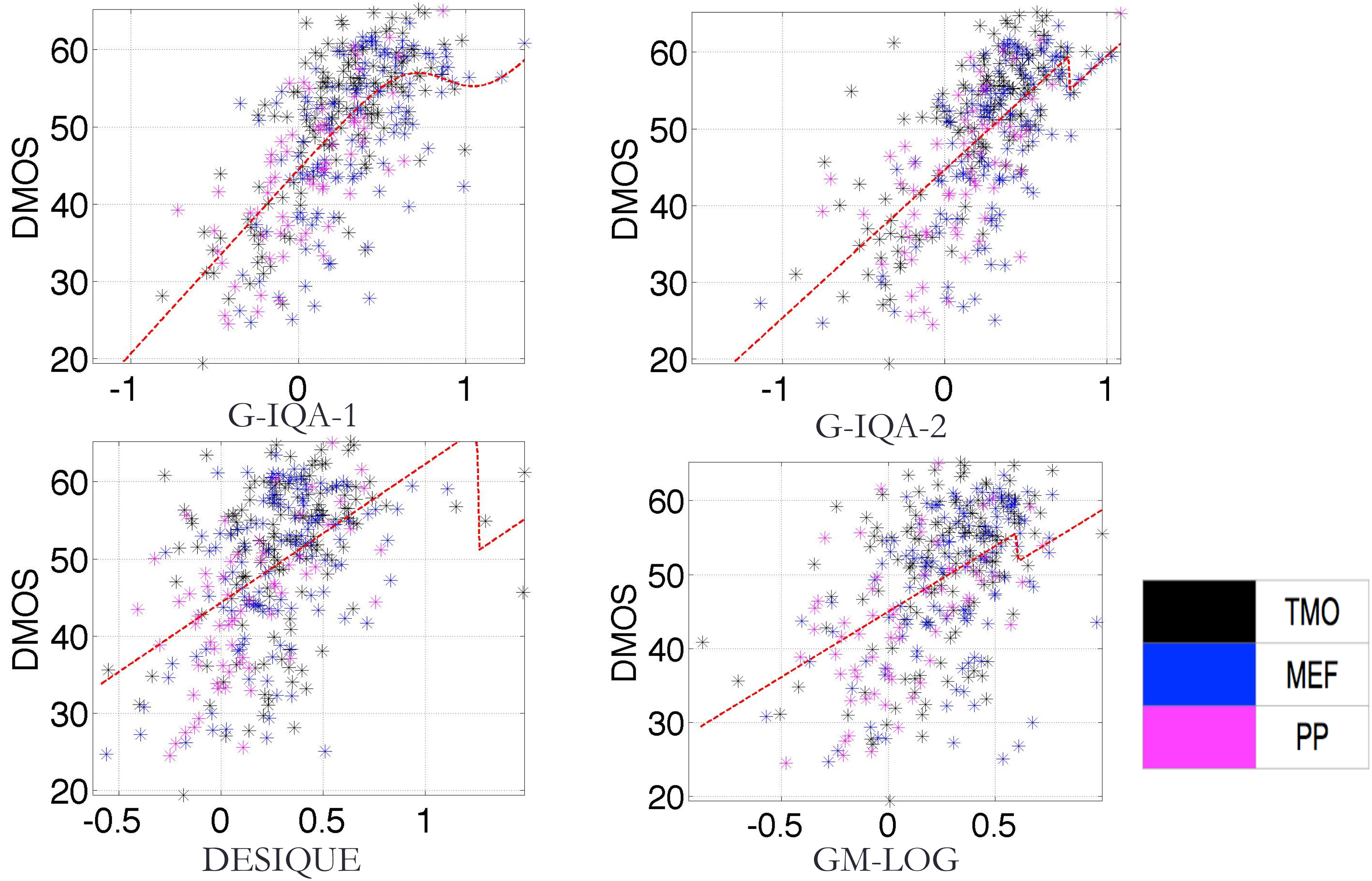

# HDR IQA: Estimating irradiance map

$$Z_{ij} = f(E_i t_j)$$

$$f^{-1}(Z_{ij}) = E_i t_j$$

$$\ln f^{-1}(Z_{ij}) = \ln(E_i) + \ln(t_j)$$

$$\ln f^{-1}(Z_{ij}) = \ln(E_i) + \ln(t_j)$$

# HDR IQA: Source Image Content

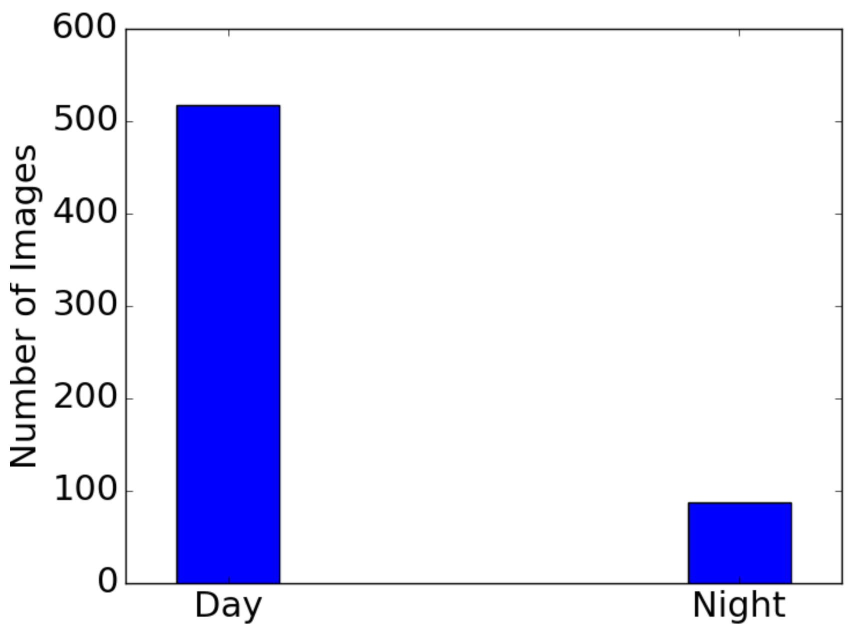


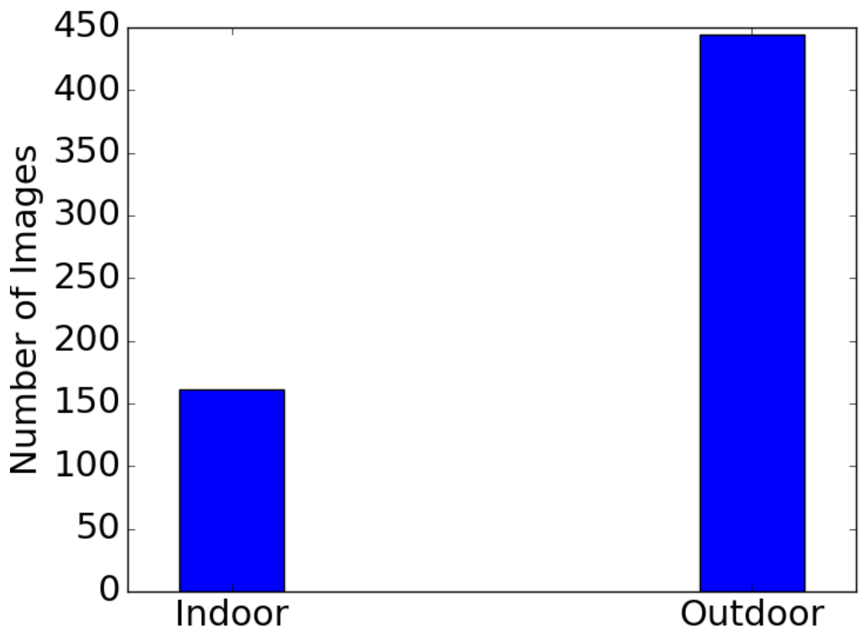

# HDR IQA: Demographics and Display parameters

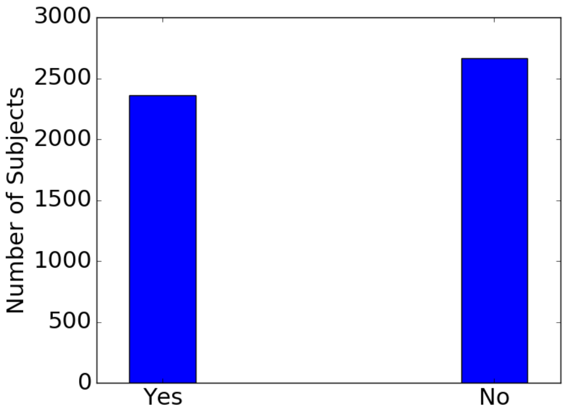


HDR familiarity

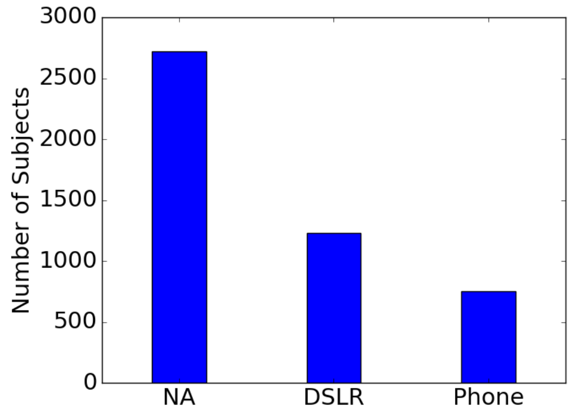


HDR Device used

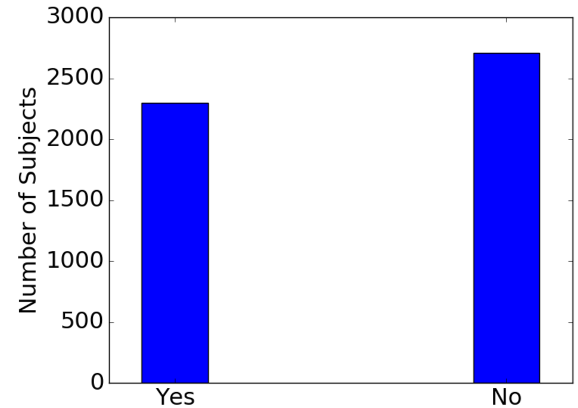


HDR software familiarity

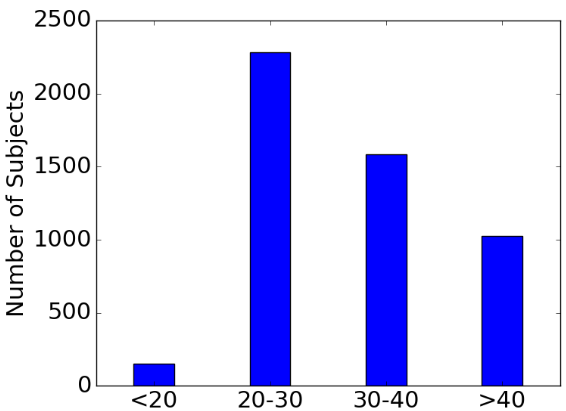


Age of subjects

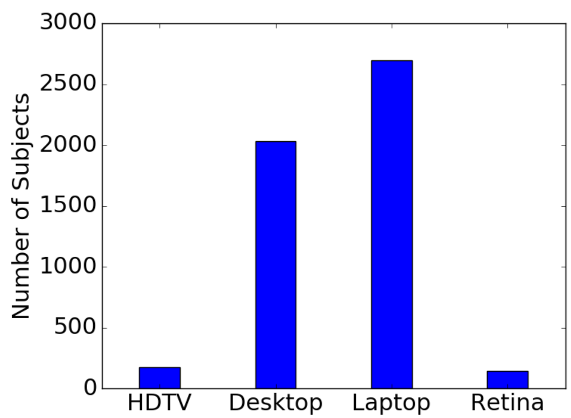


Display used

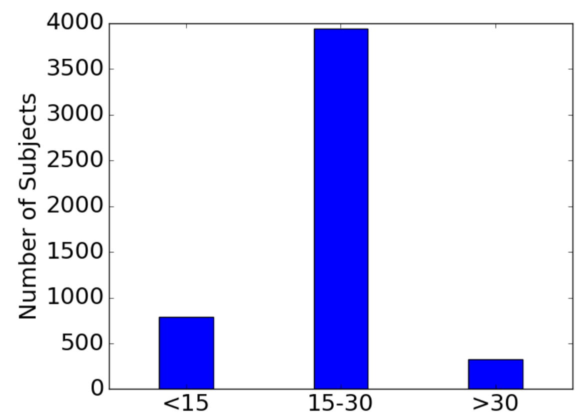


Distance from display

# HDR-IQA: Processing of the raw scores (Cont'd)

- Rating consistency:
  - Inter subject consistency : PLCC between MOS obtained by dividing the workers into two disjoint groups was **0.9677** (randomized over 25 trials)
  - Intra subject consistency: Median PLCC between individual scores and MOS values for 'Gold Standard' images was **0.8697**
  - Consistency with laboratory study: Median PLCC between individual scores and MOS values for 'Gold Standard' images in laboratory setting was **0.9466**

Back

# HDR-IQA: MOS vs. Number of subjects

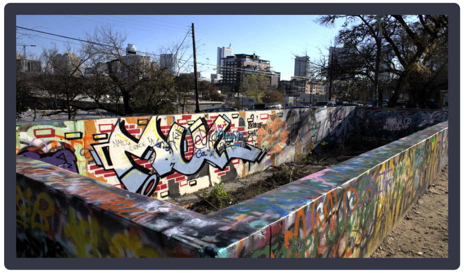



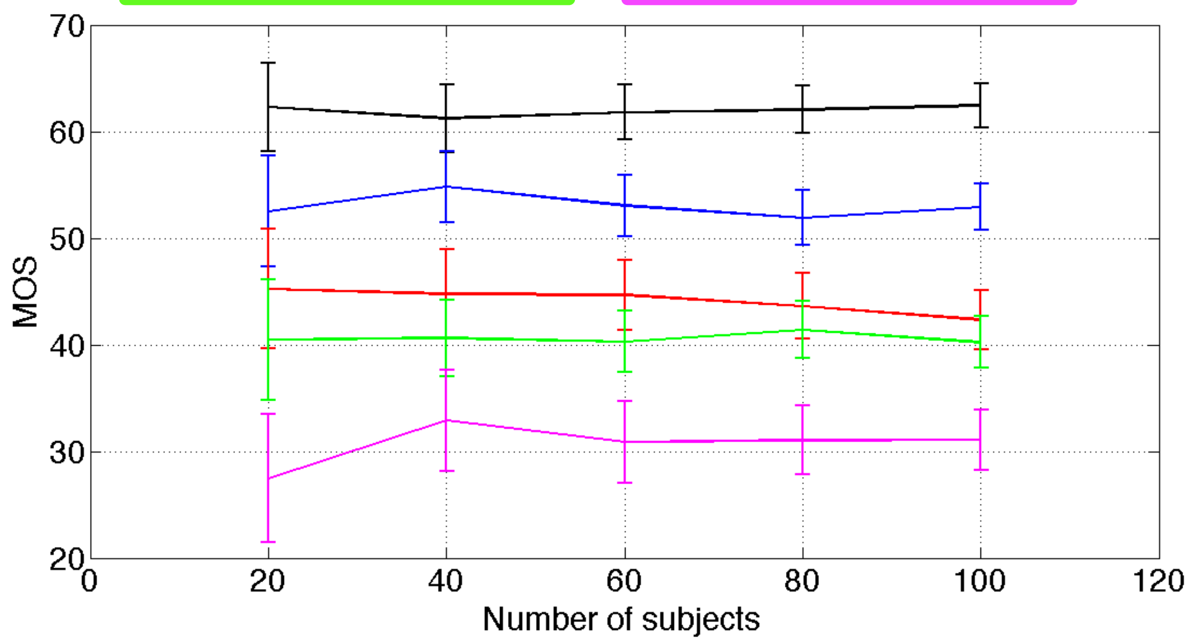


Back

# HDR-IQA: Parameter variations

1

2

3

4

5

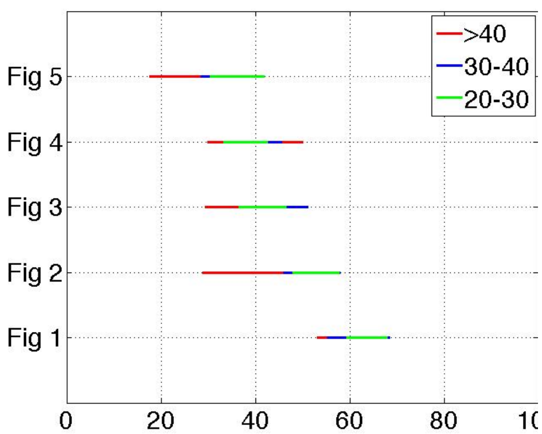


Variation with age

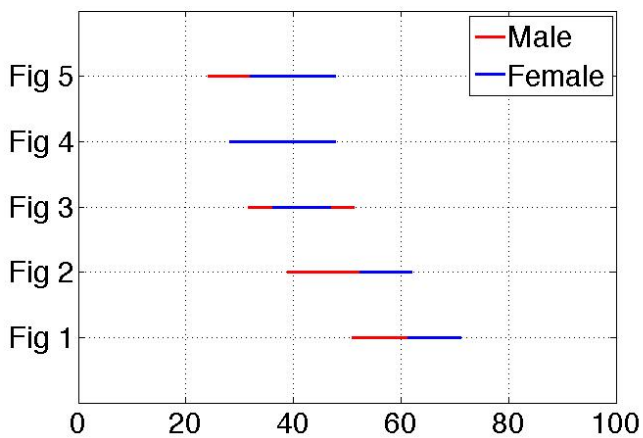


Variation with gender

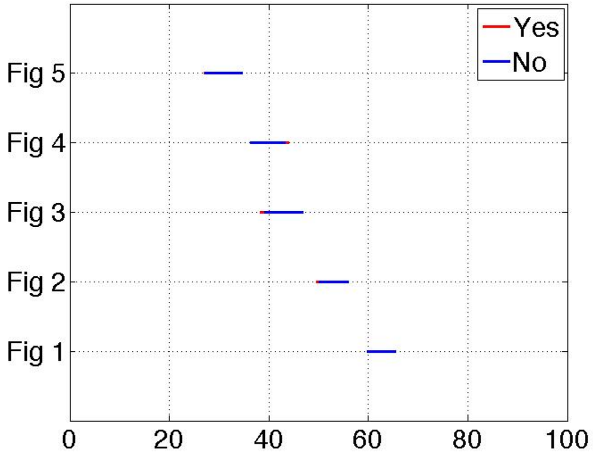


Variation with HDR awareness

Back

# HDR-IQA: Parameter variations (cont'd)

1

2

3

4

5

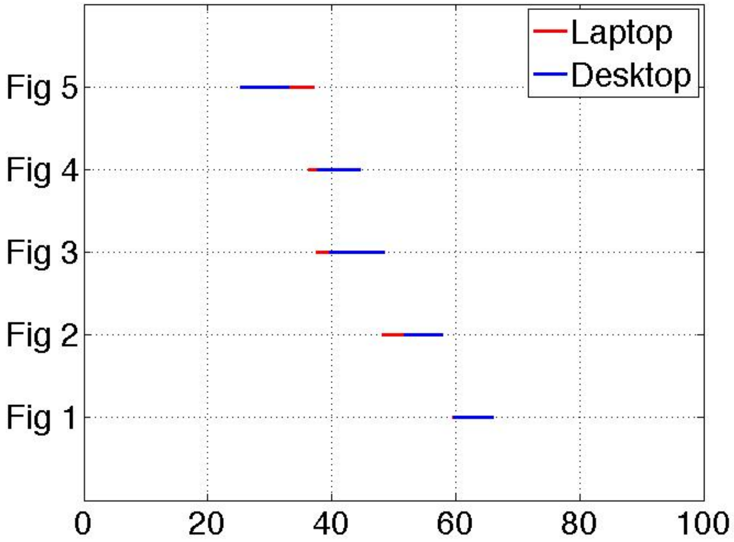


Variation with display

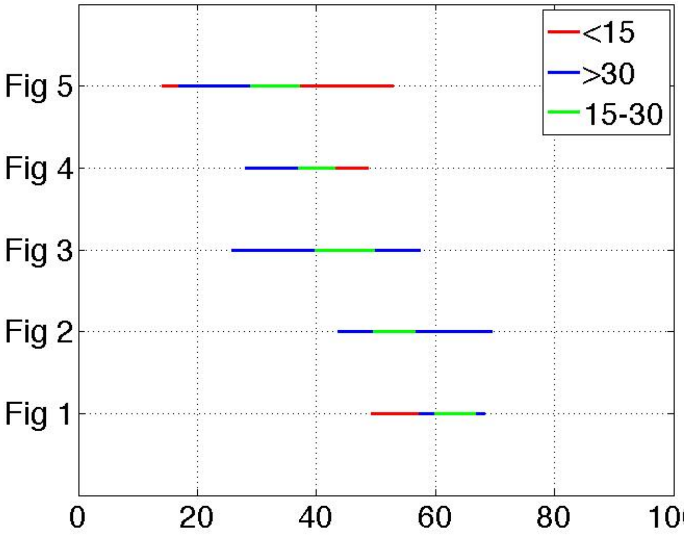


Variation with distance from display

Back